The Plant Cell, Vol. 26: 4702–4717, December 2014, www.plantcell.org

RESEARCH ARTICLES

The *dicer-like1* Homolog *fuzzy tassel* Is Required for the Regulation of Meristem Determinacy in the Inflorescence and Vegetative Growth in Maize[W][OPEN]

Beth E. Thompson,[a,1] Christine Basham,[a] Reza Hammond,[b,c] Queying Ding,[a] Atul Kakrana,[b,c] Tzuu-Fen Lee,[c] Stacey A. Simon,[c] Robert Meeley,[d] Blake C. Meyers,[c] and Sarah Hake[e]

[a] Department of Biology, East Carolina University, Greenville, North Carolina 27858
[b] Center for Bioinformatics and Computational Biology, University of Delaware, Newark, Delaware 19714
[c] Department of Plant and Soil Sciences, University of Delaware, Newark, Delaware 19711
[d] Pioneer, A Dupont Company, Johnston, Iowa 50131
[e] Plant Gene Expression Center and University of California-Berkeley, Albany, California 94710

ORCID ID: 0000-0003-3436-6097 (B.C.M.)

Plant architecture is determined by meristems that initiate leaves during vegetative development and flowers during reproductive development. Maize (*Zea mays*) inflorescences are patterned by a series of branching events, culminating in floral meristems that produce sexual organs. The maize *fuzzy tassel* (*fzt*) mutant has striking inflorescence defects with indeterminate meristems, fasciation, and alterations in sex determination. *fzt* plants have dramatically reduced plant height and shorter, narrower leaves with leaf polarity and phase change defects. We positionally cloned *fzt* and discovered that it contains a mutation in a *dicer-like1* homolog, a key enzyme required for microRNA (miRNA) biogenesis. miRNAs are small noncoding RNAs that reduce target mRNA levels and are key regulators of plant development and physiology. Small RNA sequencing analysis showed that most miRNAs are moderately reduced in *fzt* plants and a few miRNAs are dramatically reduced. Some aspects of the *fzt* phenotype can be explained by reduced levels of known miRNAs, including miRNAs that influence meristem determinacy, phase change, and leaf polarity. miRNAs responsible for other aspects of the *fzt* phenotype are unknown and likely to be those miRNAs most severely reduced in *fzt* mutants. The *fzt* mutation provides a tool to link specific miRNAs and targets to discrete phenotypes and developmental roles.

INTRODUCTION

Plant development is dependent on the activity of meristems, groups of indeterminate, self-renewing cells that initiate new organs. Maintenance of the balance between organ initiation at the periphery and self-renewal in the central stem cells is critical for plant growth (Steeves and Sussex, 1989). The shoot apical meristem initiates leaf primordia during vegetative development. As the plant becomes reproductive, leaf primordia become smaller and axillary branch meristems, in the axils of leaves, become more prominent. Ultimately, inflorescence meristems are formed that will produce flowers. Meristems are considered indeterminate if the central stem cells are maintained during the production of meristem or organ primordia, whereas meristems are considered determinate if the central stem cells are consumed, as in a floral meristem.

Maize (*Zea mays*) produces two inflorescences, the tassel and the ear, which produce male and female flowers, respectively. The tassel is the product of the apical inflorescence meristem, while the ear is the product of an axillary meristem. In both the tassel and the ear, the inflorescence meristem initiates secondary and higher order meristems, culminating in the formation of floral meristems. The imposition of determinacy on the higher order meristems determines inflorescence architecture.

MicroRNAs (miRNAs) are key regulators of meristem fate and function in maize and other plants. In maize, *tasselseed4* (*ts4*), which encodes miR172e, is required for meristem determinacy in multiple higher order meristems, in addition to playing a role in sex determination. *ts4*/miR172e represses two *AP2*-like genes, *ids1* and *sid1* (Chuck et al., 2007b, 2008), a regulatory module that is conserved in *Arabidopsis thaliana* and rice (*Oryza sativa*) (Aukerman and Sakai, 2003; Lee and An, 2012). miR156 is required for leaf suppression in the inflorescence and plays a key role in determining the meristem and leaf boundary (Chuck et al., 2010). The dominant mutant *Corngrass1* (*Cg1*), which is caused by the overexpression of miR156, has a fasciated inflorescence meristem, indicating that miR156 also plays a role in stem cell homeostasis (Chuck et al., 2007a).

miRNAs have key roles in vegetative development. The balance between miR156 and miR172 is critical to determine the switch from vegetative to reproductive development, also known as phase change, in maize, *Arabidopsis*, and other plants (Wu and Poethig, 2006; Chuck et al., 2007a, 2011; Poethig, 2013). miR165 and miR166 repress class III homeodomain-leucine zipper transcription factors to regulate abaxial/adaxial leaf polarity (McConnell et al., 2001; Juarez et al., 2004).

[1] Address correspondence to thompsonb@ecu.edu.
The author responsible for distribution of materials integral to the findings presented in this article in accordance with the policy described in the Instructions for Authors (www.plantcell.org) is: Beth Thompson (thompsonb@ecu.edu).
[W] Online version contains Web-only data.
[OPEN] Articles can be viewed online without a subscription.
www.plantcell.org/cgi/doi/10.1105/tpc.114.132670

miRNAs are small noncoding RNAs of 20 to 22 nucleotides in length that posttranscriptionally repress gene expression in plants and animals (Bushati and Cohen, 2007; Bartel, 2009; Chen, 2009; Voinnet, 2009; Krol et al., 2010). miRNA genes are transcribed by RNA polymerase II as long, primary microRNA (pri-miRNA) transcripts that contain one or more hairpin structures (Xie et al., 2005). The pri-miRNA undergoes two sequential processing events to generate the mature miRNA. The pri-miRNA is cleaved to liberate the hairpin (60 to 80 nucleotides in animals, more variable in plants) and generate the precursor microRNA (pre-miRNA). The pre-miRNA is then cleaved to release a small RNA duplex, consisting of the miRNA and its complement, the miRNA*. In plants, processing of both the pri-miRNA and pre-miRNA occurs in the nucleus, primarily by the RNA endonuclease DICER-LIKE1 (DCL1) (Kurihara and Watanabe, 2004). In *Arabidopsis*, DCL1 also requires additional protein partners for efficient and accurate miRNA processing, including the conserved double-stranded RNA binding protein HYPONASTIC LEAVES1 (HYL1), a zinc finger protein, SERRATE (SE) (Vazquez et al., 2004; Yang et al., 2006), and a second RNA binding protein, TOUGH (TGH) (Ren et al., 2012). The forkhead protein DAWDLE (DDL) and the cap binding proteins CPB80/ABH1 and CBP-20 are also required for pri-miRNA processing (Gregory et al., 2008; Laubinger et al., 2008; Yu et al., 2008). Finally, plant miRNAs are methylated by HUA ENHANCER1 (HEN1), a modification that stabilizes miRNAs (Yu et al., 2005). In *Arabidopsis* a related enzyme, DCL4, can also process some miRNAs, in particular newly evolved miRNAs with hairpins of high degrees of complementarity (Rajagopalan et al., 2006; Fahlgren et al., 2007; Ben Amor et al., 2009).

miRNAs repress target mRNAs by two major mechanisms: mRNA cleavage and translational inhibition (Bartel, 2004). The mature miRNA is incorporated into the RNA-induced silencing complex and guides it to mRNAs containing miRNA complementary sequences. Most plant miRNAs have nearly perfect complementarity with target mRNAs and cleave their targets, although increasing evidence suggests that translational inhibition is also widespread (Brodersen et al., 2008). Target cleavage requires the endonuclease ARGONAUTE1 (Vaucheret et al., 2004), and translational inhibition takes place on the endoplasmic reticulum, although the exact mechanism is still unknown (Li et al., 2013).

The key role of miRNAs during development is underscored by the broad range of developmental defects in miRNA biogenesis mutants. For example, null alleles of *Arabidopsis DCL1* are embryonic lethal, and hypomorphic alleles have defects in integument, ovule, and floral development (Schauer et al., 2002). In rice, strong *DCL1* RNA interference knockdowns result in developmental arrest, while weak knockdowns exhibit defects in plant growth, shoot, root, and leaf development (Liu et al., 2005). In addition, *Arabidopsis* mutants in other miRNA biogenesis enzymes, including *hyl1*, *se*, *tgh*, *ddl*, *abh1*, and *hen1*, have pleiotropic developmental defects, presumably due to the misregulation of miRNA target mRNAs (Clarke et al., 1999; Lu and Fedoroff, 2000; Hugouvieux et al., 2001; Prigge and Wagner, 2001; Chen et al., 2002; Calderon-Villalobos et al., 2005; Morris et al., 2006; Yang et al., 2006).

We isolated a maize mutant, *fuzzy tassel* (*fzt*), with a broad range of vegetative and reproductive defects. *fzt* mutants have particularly striking inflorescence defects, including increased indeterminacy of multiple meristems and defects in stem cell homeostasis and sex determination. *fzt* mutants also have vegetative defects, including reduced plant stature, and short narrow leaves with mild polarity defects. Positional cloning showed that *fzt* contains a mutation in DCL1, a key enzyme in the miRNA biogenesis pathway. The levels of most miRNAs are moderately reduced in *fzt* mutants; however, a few miRNAs are more dramatically reduced, suggesting that developmental defects in the *fzt* mutant are caused by reduced levels of a subset of miRNAs and the upregulation of specific miRNA-targeted mRNAs.

RESULTS

fzt Is Required during Vegetative and Reproductive Development

fzt was isolated by screening an M2 population of A619 ethyl methanesulfonate (EMS)-mutagenized plants. The mutant was backcrossed to A619 a minimum of three times prior to analysis; analysis was done in the A619 inbred background unless noted otherwise. *fzt* is recessive, 100% penetrant, and has striking reproductive defects and reduced plant stature (Figure 1; Supplemental Figure 1). We also backcrossed the *fzt* mutation to Mo17 and B73 a minimum of three times for analysis. *fzt* phenotypes are qualitatively similar in all inbred backgrounds examined; however, some defects appear more severe in the Mo17 and B73 inbred backgrounds (see below).

Plant stature is dramatically reduced in *fzt* mutants. *fzt* plants are less than one-third the height of normal sibling plants (Figure 1A; Supplemental Figure 1A). We counted the number of leaves, including the first juvenile leaves, to determine if this loss of stature was due to short or missing internodes. Whereas normal siblings produced on average 15 leaves, *fzt* mutants produced only an average of 12 leaves, suggesting that the short stature was a combination of both missing and shorter internodes (Supplemental Figure 1B). To confirm this finding, we quantified the number and length of internodes at maturity and found that normal plants had an average of 10.5 nodes per plant whereas *fzt* plants had an average of only 8 nodes per plant (Supplemental Figure 1C). We also measured internode length in *fzt* and normal plants. *fzt* plants had significantly shorter internodes, except for the top-most internode of *fzt* plants (internode 8) (Supplemental Figure 1D).

Leaf size was also reduced in *fzt* plants; *fzt* leaves were only about two-thirds the length and less than one-half the width of normal leaves (Supplemental Figures 1E and 1F). To determine if reduced leaf size was due to a decrease in cell size or cell number, we counted total epidermal cell number per unit area as a measure of cell size; increased cell number per unit area would be indicative of decreased cell size in *fzt* plants. Surprisingly, we found that *fzt* plants had a slight decrease in cell number per unit area compared with normal siblings, suggesting that cell size is slightly increased in *fzt* leaves compared with normal siblings (Supplemental Figure 1G). Thus, the decrease in leaf size is likely

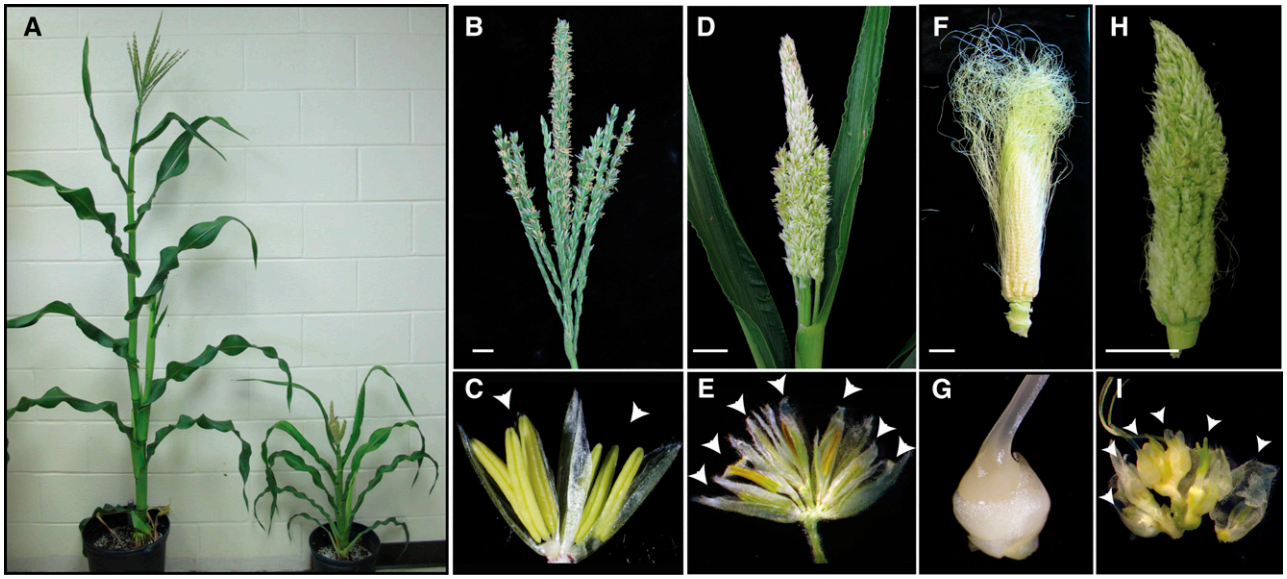

Figure 1. *fzt* Mutants Have Severe Vegetative and Inflorescence Defects.

(A) Normal sibling (left) next to an *fzt* mutant (right). *fzt* mutants are much shorter than normal siblings.
(B) Normal tassel.
(C) A normal tassel spikelet containing two florets. Glumes have been removed to expose the florets.
(D) *fzt* mutant tassel. Spikelets lack recognizable glumes.
(E) *fzt* tassel spikelet containing extra florets. *fzt* florets contain abnormal stamens that do not shed pollen and other abnormal floral organs.
(F) Normal ear.
(G) Dissected ear spikelet from a normal ear contains a single floret.
(H) *fzt* ear contains few silks and abnormal bracts and is sterile.
(I) *fzt* ear spikelet contains extra florets, abnormal floral organs, and undeveloped stamens.
White arrowheads indicate florets. Bars = 2 cm.

due to a decrease in total cell number rather than decreased cell size.

The reproductive defects in *fzt* plants are particularly striking (Figures 1B to 1I). In normal maize plants, tassels produce staminate flowers and ears produce pistillate flowers, due to the abortion of pistils in the tassel and stamen arrest in the ear. In addition to sex organs, maize florets contain grass-specific organs, including lodicules, palea, and lemma. Lodicules have homology to petals (Ambrose et al., 2000), and palea and lemma are bract-like organs. Spikelets are produced in pairs; each spikelet consists of two florets enclosed by two bracts, called glumes (Figure 1C). In ears, one of the two florets aborts (Figure 1G). In *fzt* plants, both male and female inflorescences exhibit multiple defects resulting in complete sterility. *fzt* tassels often produce extra spikelets, and the spikelets contain more than two florets (Figure 1E). *fzt* tassel florets make an excess of palea/lemma-like organs, and the stamens are small, undeveloped, and never shed pollen. *fzt* spikelets also lack recognizable glumes, resulting in exposed floral organs and their "fuzzy" appearance (Figure 1D). On average, *fzt* tassels produce only one-half the number of tassel branches as normal siblings (5 branches in *fzt* versus 9.5 branches in normal siblings) (Supplemental Figure 1H). *fzt* tassels occasionally produce silks, indicating that carpel abortion is defective.

The *fzt* mutation also severely affects ear development. *fzt* ear spikelets are enclosed by bracts that morphologically resemble tassel glumes and contain extra florets (Figure 1I). Ear florets also make extra palea-like organs and often contain immature stamens, indicating that *fzt* is required for multiple aspects of sex determination in the ear.

We observed similar phenotypes when *fzt* was introgressed into the Mo17 and B73 inbred backgrounds (Supplemental Figure 2). The *fzt* mutation had similar effects on plant stature in all three inbred backgrounds (Supplemental Figures 2A, 2B, 2J, and 2K); however, the inflorescence defects were more severe in Mo17 and B73 than in the A619 inbred. *fzt*[Mo17] and *fzt*[B73] tassels were highly branched and formed no recognizable florets, although tassel "spikelets" produced lemma/palea-like organs and a few undeveloped and abnormal stamens (Supplemental Figures 2D, 2G, 2M, and 2N). *fzt*[B73] ears were highly branched and contained many immature meristems at maturity. Almost no floral organs were produced, except for rare immature and abnormal stamens (Supplemental Figures 2F, 2H, and 2I). *fzt*[Mo17] plants generally lacked ears.

fzt Contains a Mutation in DCL1

To gain insight into the molecular underpinnings of the *fzt* phenotype, we positionally cloned the gene. *fzt* mapped to the short arm of chromosome 1 between the simple sequence repeat markers bnlg1124 and umc1292. We developed new

polymorphic markers to narrow the *fzt*-containing region to an ~3.2-centimorgan region, which included 33 predicted genes, 26 of which had functional annotations (gene predictions were obtained from the filtered gene set of the maize B73 RefGen_v2) (Figure 2A). One gene in this interval, *dcl1*, stood out as a particularly strong candidate. DCL1 is a key enzyme required for miRNA biogenesis in *Arabidopsis* and other plant species and is broadly expressed during development (Sekhon et al., 2011). Given the well-established role of miRNAs in many developmental processes, including the regulation of meristem determinacy in maize, a mutation in *dcl1* seemed likely to underlie the pleiotropic phenotypes of *fzt*.

DCL proteins contain several conserved domains, including a bipartite helicase domain, a DUF283 domain that was recently defined as a novel RNA binding motif (Qin et al., 2010), two RNase III domains (RNase IIIa and RNase IIIb), and two double-stranded RNA binding domains (Figure 2B). The *dcl1* locus corresponds to gene model GRMZM2G040762. To assemble the full *dcl1* genomic sequence and predict a full-length coding sequence, we assembled maize BAC sequences and used similarity with the rice and *Arabidopsis* DCL1 protein sequences to predict a full-length maize DCl1 protein (1929 amino acids) and corresponding coding sequence (5790 nucleotides) (see Methods). We sequenced the predicted *dcl1* coding region from *fzt* and A619 plants and found a G-to-A mutation in *fzt* mutants corresponding to exon 17 and predicted to cause an S-to-N substitution in the RNase IIIa domain (Figure 2B; Supplemental Figure 3).

To generate additional alleles and confirm that we isolated the correct gene, we conducted a noncomplementation screen in which Mo17 EMS-mutagenized pollen was crossed onto *fzt* heterozygotes and the resulting progeny were scored for *fzt* phenotypes. We found one plant with the *fzt* phenotype that contained a G-to-A mutation in exon 19, which is predicted to introduce a premature stop codon and truncate DCL1 by 39 amino acids. The *fzt/fzt-EMS* plant was sterile, and we were unable to recover the new allele for further experiments. We obtained four additional *dcl1* alleles (*dcl1-mum1* to *dcl1-mum4*) through reverse genetics resources (Bensen et al., 1995). Three alleles (*dcl1-mum2* to *dcl1-mum4*) contain Mu insertions in the

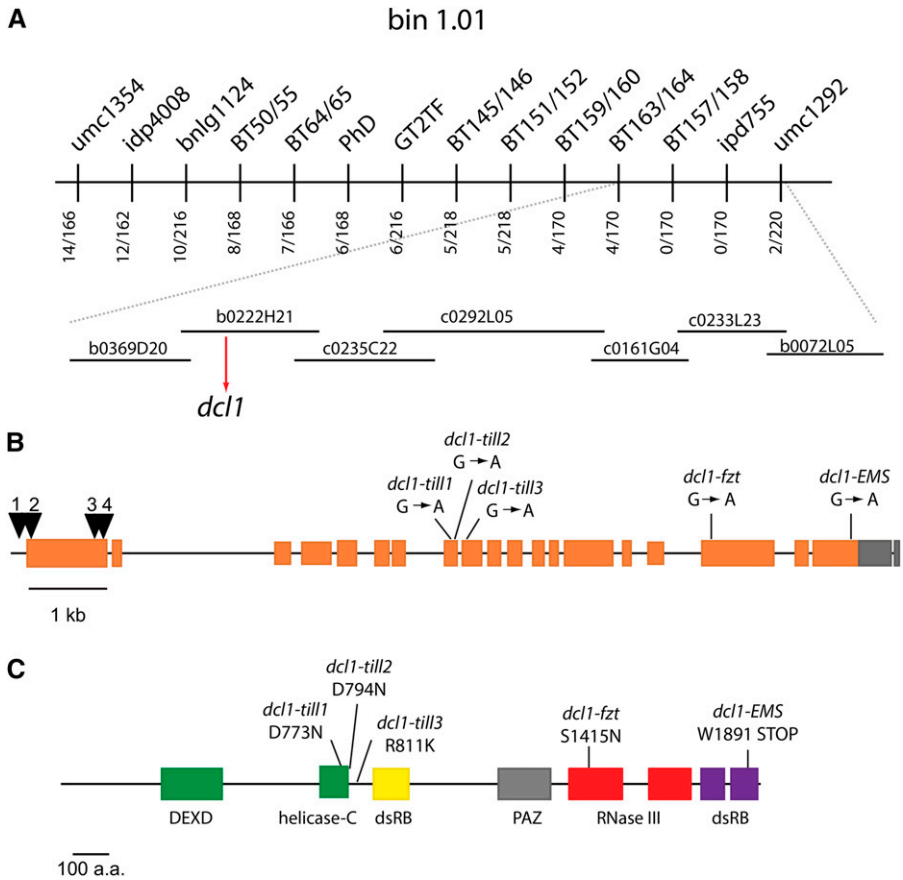

Figure 2. *fzt* Contains a Mutation in *dcl1*.

(A) Mapping data for *fzt*.

(B) Genomic region of *dcl1* with mutant alleles indicated. Black triangles indicate insertion sites of Mutator transposon insertions (*dcl1-mum1-4*). Orange boxes indicate protein-coding exons, and gray boxes indicate 3′ untranslated regions.

(C) Schematic of the DCL1 protein with conserved domains indicated. The predicted effects of the mutant alleles on the DCL1 protein are indicated. a.a., amino acids.

protein-coding region of exon 1 and are likely null alleles; all three alleles fail to complement *fzt*. Based on *dcl1* null phenotypes in *Arabidopsis*, we hypothesized that null alleles of *dcl1* are embryonic lethal. We examined the self-progeny of *dcl1-mum3* heterozygotes, one-quarter of which are predicted to be *dcl1-mum3* homozygotes. We found that 49 of 172 (28.4%) seeds lacked recognizable embryos, and all seeds with a recognizable embryo contained at least one normal *dcl1* allele (Supplemental Figure 4B). Thus, *dcl1-mum3* homozygotes are indeed early embryonic lethal. Homozygous *dcl1-mum2* and *dcl1-mum4* plants were never recovered, suggesting that these alleles are also embryonic lethal. We also asked if *dcl1-mum3* is transmitted normally by analyzing progeny from reciprocal crosses. The *dcl1-mum3* allele is inherited in the expected Mendelian ratios ($P > 0.1$ in χ^2 test), indicating that *dcl1-mum3* is transmitted normally by both the male and female gametophytes (Supplemental Figure 4C). Based on these results, we conclude that *fzt* is a *dcl1* allele, and we refer to our allele as *dcl1-fzt*. We also obtained three *dcl1* tilling alleles from the Maize Tilling Project (Till et al., 2004) that contained nonsilent point mutations in or near the helicase domain (Figures 2B and 2C). Interestingly, plants homozygous for these alleles were phenotypically normal and complemented the *fzt* mutation, suggesting that the helicase domain may not be critical for DCL1 function in an otherwise normal genetic background, although it is also possible that these mutations do not impair helicase function.

dcl1-fzt Mutants Are Defective in miRNA-Regulated Processes

miRNAs have well-known roles in plant development (Bartel, 2009; Chen, 2009; Rubio-Somoza and Weigel, 2011). Given that *dcl1-fzt* carries a mutation in a key enzyme required for miRNA biogenesis, we predicted that *dcl1-fzt* mutants would have reduced miRNA levels. Therefore, we examined *dcl1-fzt* mutants for defects in several miRNA-regulated processes.

miRNA regulation is required to regulate meristem determinacy in the inflorescence. The *dcl1-fzt* inflorescence defects resemble those of the *ts4* mutant, which is caused by a loss-of-function mutation in miR172e. Reduced miR172e expression leads to the loss of meristem determinacy and sex determination defects (Chuck et al., 2007b, 2008). To more closely examine *dcl1-fzt* mutants for these defects, we examined early inflorescence development by scanning electron microscopy. In normal plants, the inflorescence meristem (IM) gives rise to ordered rows of spikelet pair meristems (SPMs). Each SPM gives rise to two spikelet meristems (SMs), which in turn give rise to two floral meristems (FMs), which produce the floral organs. Development in the tassel and ear is similar, except that in the tassel the IM also initiates branch meristems (BMs) and in the ear only one floret per spikelet develops to maturity. In *ts4* mutants, SPMs initiate extra spikelets and SMs initiate extra FMs (Chuck et al., 2007b). We observed similar defects in *dcl1-fzt* plants (Figure 3). The SPMs of *fzt* mutants initiated more than two SMs (asterisks in Figure 3J) and the SMs of *fzt* mutants persisted (arrow in Figure 3L), initiating more than the normal two FMs (asterisks in Figure 3L). We also found that miR172e was substantially reduced in *dcl1-fzt* mutants compared with normal controls (see below), consistent with the observed meristem determinacy defects.

Normal meristems grow as a single apex by balancing stem cell growth with the rate of primordium initiation. Meristems that lose this homeostasis broaden and become fasciated (Aichinger et al., 2012; Pautler et al., 2013). We consistently noted fasciation in *dcl1-fzt* IMs (Figure 3H; Supplemental Figure 5). The broadened tip produced many more meristems than normal. We also observed fasciation in the BMs (Figure 3H, arrowhead). Finally, SPMs were not initiated in ordered rows and were irregular in shape and size (Figures 3E and 3G; Supplemental Figure 5). These defects are not observed in the *ts4* mutant, suggesting that miRNAs in addition to miR172e are reduced in the *dcl1-fzt* mutant and have key roles in meristem homeostasis and determinacy.

miRNAs also have well-established roles in vegetative development. Normal maize leaves have a ligule on the adaxial surface and distinct hairs on the adaxial and abaxial surfaces. Mutations in the miR166 binding site of *Rolled-leaf1* cause the adaxialization of leaf surfaces, resulting in curled leaves and abaxial ligules (Juarez et al., 2004). Since *dcl1-fzt* leaves did not exhibit these macroscopic polarity defects, we examined the leaves for subtle polarity defects. In normal leaves, macrohairs are restricted to the adaxial surface of leaf blades and are often used as adaxial markers. We examined the distribution of macrohairs on *dcl1-fzt* and normal leaf blades and found that *dcl1-fzt* leaves contained fewer macrohairs on the adaxial blade compared with normal siblings (Figures 4A and 4B). In addition, *dcl1-fzt* leaves contained macrohairs on the abaxial blade, while normal leaves did not (Figures 4C and 4D). Interestingly, this defect was more severe in the Mo17 inbred background (Figures 4A to 4D) than in the A619 background (Supplemental Figure 6), in which abaxial macrohairs were restricted to the leaf margins and were not present throughout the blade (Supplemental Figure 6D).

Vascular bundles are also polarized, with the xylem positioned at the adaxial pole and phloem positioned at the abaxial pole. We examined the polarity of vascular bundles in *dcl1-fzt* [Mo17] and normal sibling plants in cross sections. We found that *dcl1-fzt* [Mo17] mutants had subtle defects in vascular organization. The xylem was more disorganized in *dcl1-fzt* [Mo17] mutants than in normal siblings and extended farther toward the abaxial pole than normal (Figures 4E and 4F). Together, these results are consistent with mild leaf polarity defects in *dcl1-fzt* mutants, in which the abaxial surface acquired adaxial characteristics.

Phase change from the juvenile to adult life phase is another well-known miRNA-regulated process in plants and is controlled by the antagonistic activities of miR156 and miR172 (Chuck et al., 2007a; Poethig, 2013). Juvenile and adult leaves make distinct epicuticular waxes, which can be distinguished by toluidine blue staining: juvenile cells stain violet in color, while adult cells stain blue. We found that in the A619 inbred background, *dcl1-fzt* mutants begin making adult waxes about one leaf later than normal siblings (Supplemental Figure 7). Combined with the node number data (Supplemental Figure 1C), this indicates that, on average, *dcl1-fzt* [A619] plants gain one juvenile internode and lose four adult internodes. By contrast, in the Mo17 inbred background, *dcl1-fzt* mutants begin making

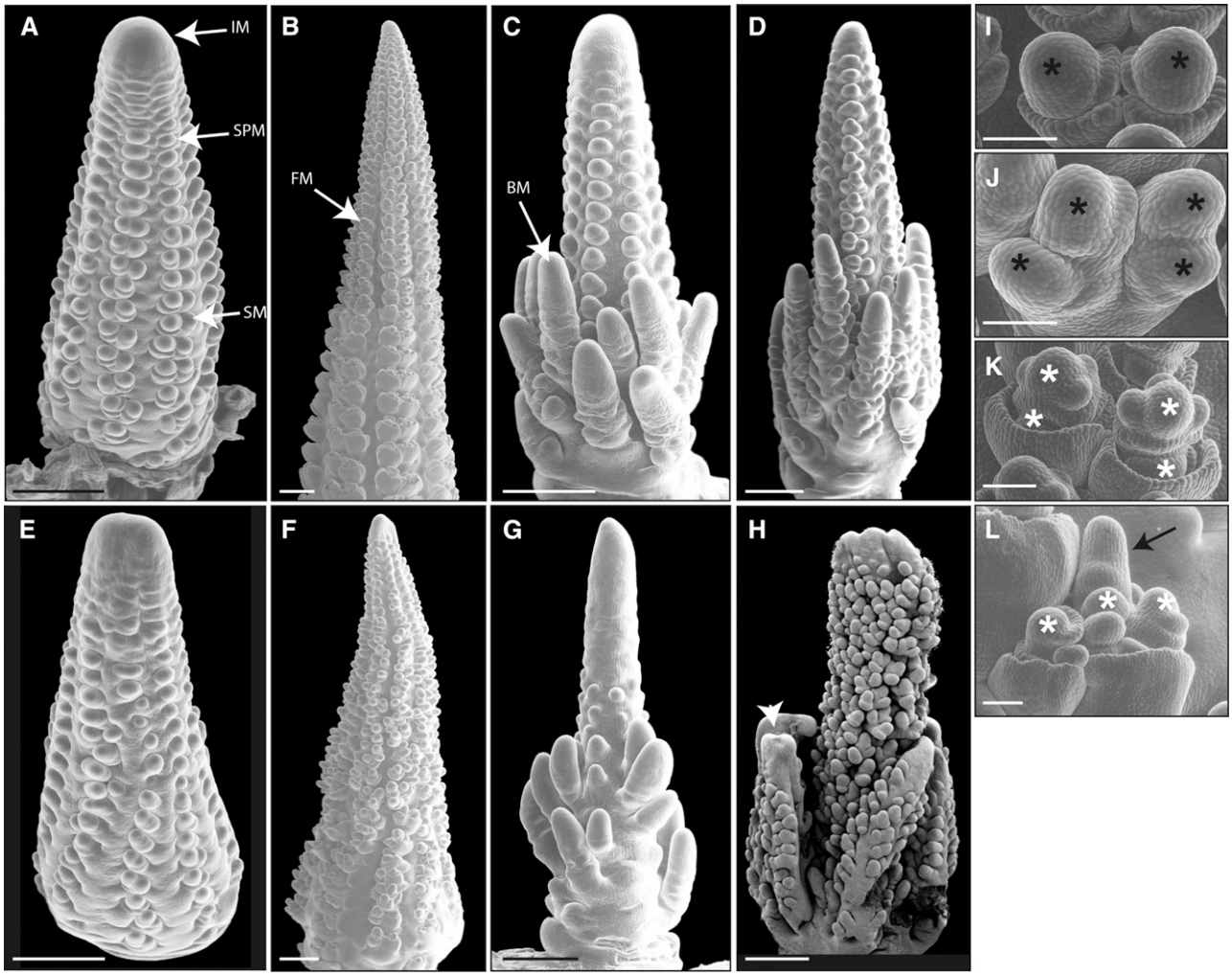

Figure 3. *dcl1-fzt* Inflorescences Make Abnormal Meristems.

(A) to **(H)** Scanning electron micrographs of normal (**[A]** to **[D]**) and *dcl1-fzt* mutant (**[E]** to **[H]**) inflorescences. A young normal ear **(A)** is compared with a young *dcl1-fzt* mutant ear **(E)**. *dcl1-fzt* IMs are flattened and broader than normal, indicating mild fasciation. *dcl1-fzt* SPMs are enlarged and not initiated in ordered rows. An older normal ear **(B)** is compared with a *dcl1-fzt* older ear **(F)**. Normal tassels (**[C]** and **[D]**) are compared with *dcl1-fzt* mutant tassels (**[G]** and **[H]**). The white arrowhead in **(H)** indicates fasciated BMs.

(I) Normal spikelet pair contains two SMs. Each SM is subtended by a glume.

(J) *fzt* mutant spikelet "pair" contains extra SMs, and not all SMs are subtended by glumes.

(K) Normal spikelet pair during floral development. Each spikelet consists of an upper FM and a lower FM. Floral organs are initiated in a stereotypical, ordered manner.

(L) Older *fzt* mutant spikelet pair. Spikelets initiate extra FMs. Floral development is abnormal, and floral organs are not initiated properly. An indeterminate branch-like meristem persists (black arrow).

Black asterisks indicate SMs, and white asterisks indicate FMs/developing florets. Bars in **(A)** to **(H)** = 0.5 mm; bars in **(I)** to **(L)** = 100 μm.

adult leaf waxes approximately one leaf earlier than normal siblings (Supplemental Figure 7). While initially it seems paradoxical that *dcl1-fzt* has opposite effects on phase change depending on the inbred background, this is not necessarily unexpected, given that the timing of phase change is regulated by the opposing activities of miR156 and miR172 and their target genes. Slight changes in the relative levels of these genes could shift the balance of downstream target genes and the timing of phase change. An alternative explanation for the apparent background effects on phase change is incomplete introgression. A619 and Mo17 flower at different times, with Mo17 up to 2 weeks later than A619, and thus the early phase change in *dcl1-fzt* [Mo17] plants could be due to residual A619 alleles that promote early phase change. We think that this hypothesis is unlikely for two reasons. First, we compared *dcl1-fzt* [Mo17] with normal siblings; both groups should have similar amounts of residual A619 DNA. Second, normal siblings from both the A619 and Mo17 introgressions transition at the same

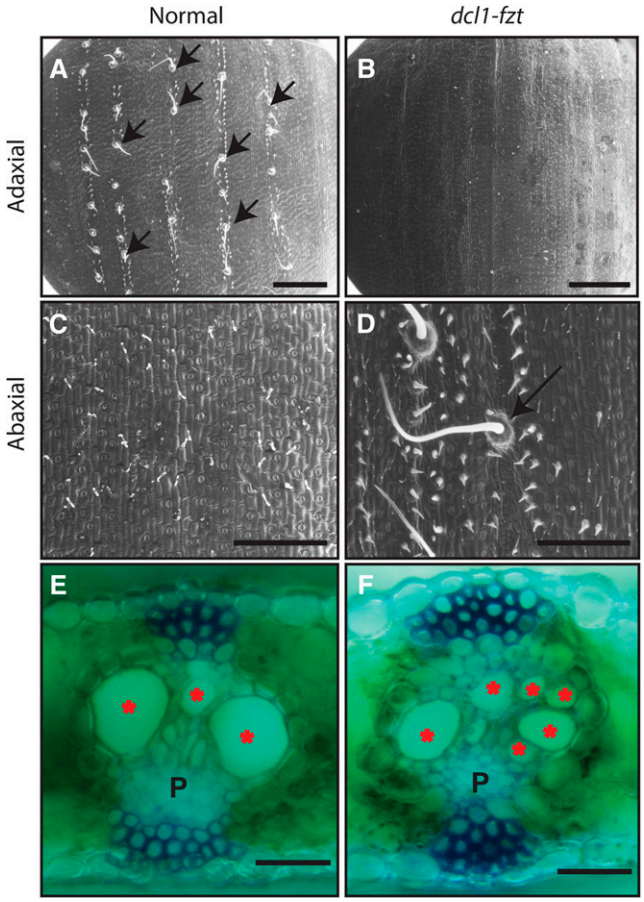

Figure 4. *dcl1-fzt* Is Required for Normal Leaf Cell Differentiation.

Macrohairs (arrows) are present on the adaxial surface of a normal leaf blade **(A)** but absent from the abaxial surface **(C)**. *dcl1-fzt* [Mo17] contains fewer macrohairs on the adaxial surface **(B)**, but macrohairs are present on the abaxial surface **(D).** Vascular polarity is also perturbed in *dcl1-fzt* [Mo17] mutants (**[E]** and **[F]**). A normal vascular bundle is shown in **(E)**. Xylem cells (red asterisks) are positioned adaxially relative to the phloem cells (P). In *dcl1-fzt* [Mo17] mutants **(F)**, the xylem cells are disorganized and extend farther toward the abaxial pole than normal. Bars in **(A)** and **(B)** = 1 mm; bars in **(C)** and **(D)** = 400 μm; bars in **(E)** and **(F)** = 50 μm.

point in development (leaf 5 to 6), whereas *dcl1-fzt* [Mo17] plants begin to transition two leaves before *dcl1-fzt* [A619] plants (leaf 5 in Mo17 versus leaf 7 in A619). Thus, Mo17 alleles promote an earlier transition in the presence of the *dcl1-fzt* mutation. Together, these results indicate that *dcl1-fzt* mutants have defects in known miRNA-regulated processes in plants, including meristem determinacy, leaf polarity, and phase change, consistent with decreased miRNA levels in *dcl1-fzt* mutants.

miRNA Levels Are Reduced in *fzt* Mutants

To determine the effect of the *dcl1-fzt* mutation on miRNA biogenesis, we analyzed the small RNA populations in 14-d-old seedlings and tassel primordia of *dcl1-fzt* and normal plants by deep sequencing. In total, small RNA libraries representing three biological replicates of seedlings and tassel primordia from *dcl1-fzt* and normal controls were generated and sequenced (Supplemental Table 1). The raw small RNA sequences were processed to remove adapter sequences and matched to the maize genome (AGPv2). To compare between libraries, the count/abundance of each small RNA was normalized based on the sequencing depth as reads per 10 million. We found that the small RNA profiles from normal and *dcl1-fzt* seedlings and tassel primordia are similar (Supplemental Figure 8). To determine if the *dcl1-fzt* mutation affected the accumulation of a subset of miRNAs, we compared the levels of individual miRNAs in *dcl1-fzt* seedlings and tassel primordia with normal controls. Approximately one-third of the detectable miRNAs (22 of 63 in seedlings and 14 of 45 in tassel primordia) were differentially expressed in *dcl1-fzt* mutants compared with normal controls ($P < 0.05$ and false discovery rate [FDR] < 0.05) (Figure 5; Supplemental Table 2). miRNAs are denoted as -5p or -3p to indicate from which arm of the hairpin precursor the mature miRNA is processed (Griffiths-Jones et al., 2006). Eight miRNAs were reduced in both seedlings and tassel primordia tissues, consistent with a defect in the processing of specific miRNAs (miRNAs in boldface and underlined in Figure 5). Not all miRNAs are affected to the same extent in *dcl1-fzt* mutants, suggesting a processing defect in a subset of miRNAs. For example, miR167a-d-5p was reduced 20- to 30-fold in both seedlings and tassel primordia, whereas miR160a-e,g-5p was decreased only 3- to 5-fold, and many miRNAs did not meet the statistical threshold for differential expression. We note, however, that although many miRNAs did not meet the statistical threshold for differential expression, nearly all of these "nonsignificant miRNAs" (38 of 40 in seedlings and 24 of 31 is tassel primordia) appeared to decrease in *dcl1-fzt* mutants, suggesting a broad, moderate reduction in the levels of miRNAs.

Mature miRNAs are processed from primary miRNA transcripts, and miRNA processing mutants often have increased levels of miRNA precursors (Kurihara and Watanabe, 2004; Kurihara et al., 2006; Yang et al., 2006; Laubinger et al., 2010). Therefore, we also examined the expression of pri-miRNA transcripts in *dcl1-fzt* and normal controls using RNA sequencing (RNA-seq; see below). In both seedlings and tassel primordia, ~50% of detectable miRNAs were differentially expressed between *dcl1-fzt* and normal controls ($P < 0.05$; 16 of 38 in seedlings and 20 of 39 in tassel primordia). Nearly all differentially expressed precursors were increased in *dcl1-fzt* mutants compared with normal controls (16 of 16 in seedlings and 17 of 20 in tassel primordia) (Supplemental Figure 9 and Supplemental Table 3). For approximately half of the upregulated precursors, the corresponding mature miRNA was decreased in *dcl1-fzt* mutant plants (pri-miRNAs are in boldface and underlined in Supplemental Figure 9). The molecular analysis of miRNA and pri-miRNA levels, combined with genetic analysis of the *dcl1-fzt* allele, strongly support the conclusion that *dcl1-fzt* is a hypomorphic allele and indicate that the DCL1-FZT enzyme is defective in processing a subset of miRNA precursors.

Plant miRNAs primarily regulate gene expression by promoting the cleavage and degradation of target mRNAs (Bartel, 2004). Therefore, we expect mRNAs targeted by miRNAs reduced in *dcl1-fzt* to be increased in *dcl1-fzt* plants compared with normal

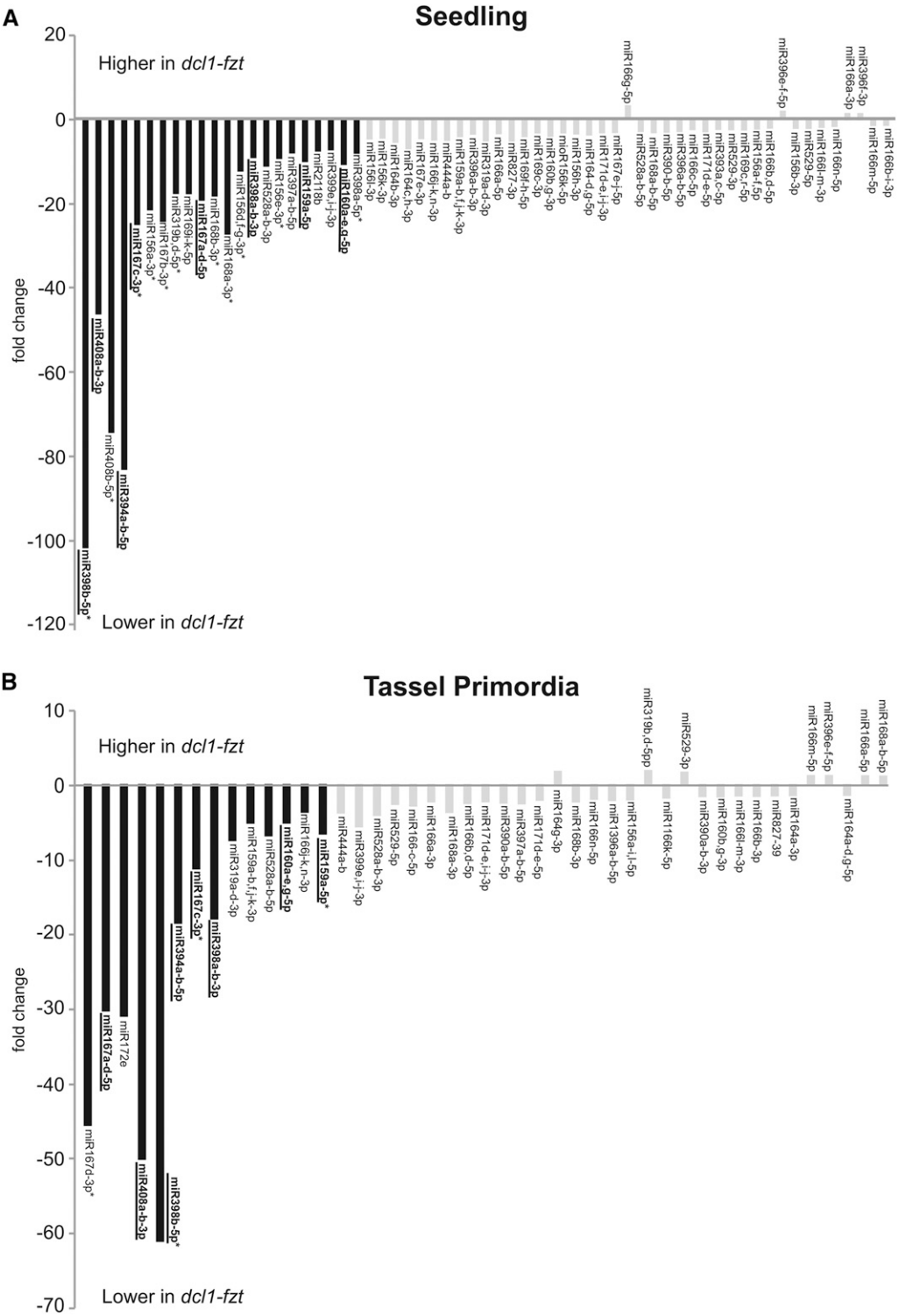

Figure 5. miRNA Levels Are Reduced in *dcl1-fzt* Mutants.

(A) Comparison of individual miRNA levels in *dcl1-fzt* and A619 seedlings.

(B) Comparison of individual miRNA levels in *dcl1-fzt* and normal sibling tassel primordia.

controls. We analyzed the transcriptome of *dcl1-fzt* and normal control plants in seedlings and tassel primordia using RNA-seq. For this analysis, we analyzed mRNAs that are predicted targets of miRNAs decreased in *dcl1-fzt* seedlings or tassel primordia (Figure 6; Supplemental Figure 10). We first analyzed the expression of all predicted target mRNAs (having a miRferno [mF] score $\leq$ 7; see Methods). In the tassel, 314 of 6343 mRNAs predicted as targets of miRNAs were differentially expressed ($P < 0.5$ and FDR < 0.05); 137 predicted target mRNAs were increased and 177 target mRNAs were decreased in *dcl1-fzt* tassel primordia compared with normal controls (Figure 6A; Supplemental Data Set 1). In seedlings, 928 of 9420 mRNAs predicted as targets of miRNAs predicted were differentially expressed: 611 predicted target mRNAs were increased and 317 target mRNAs were decreased in *dcl1-fzt* mutants (Supplemental Figure 10A and Supplemental Data Set 2). Thus, we did not observe a broad increase of miRNA target levels in *dcl1-fzt* mutants, at least at the level of the tissue used for RNA-seq libraries.

The initial target list may have included many false positives that are not in vivo miRNA targets. Therefore, we also analyzed predicted targets with mF scores $\leq$ 4, which enrich for higher confidence targets (Fahlgren et al., 2007). In the tassel, 117 predicted targets had mF scores $\leq$ 4, of which 14 showed a differential abundance ($P < 0.05$ and FDR < 0.05) between mutant and normal controls. Of these differentially expressed target mRNAs, 12 of 14 (84%) were increased in *dcl1-fzt* mutants (Figure 6B; Supplemental Data Set 3). Similarly, in the seedling, 151 predicted target mRNAs had mF scores $\leq$ 4, 26 of which were differentially expressed ($P < 0.05$ and FDR < 0.05) between mutant and normal controls. Of the differentially expressed target mRNAs, 19 of 26 (73%) were increased in *dcl1-fzt* mutants (Supplemental Figure 10B and Supplemental Data Set 4).

Many in vivo miRNA targets have mF scores > 4 due to the loose complementarity in the seed region between the miRNA and target mRNA. Therefore, we also assembled a list of high-confidence targets based on a conserved biological function with miRNA targets in other plant species, which include targets with a range of mF scores (Supplemental Tables 4 and 5). Similar to the mF-enriched targets, a small proportion (11 of 41 in tassel primordia and 17 of 51 in seedlings) of the "biologically defined" targets were differentially expressed between *dcl1-fzt* and normal controls ($P < 0.05$ and FDR < 0.05). In the tassel, 10 of 11 of the differentially expressed biologically defined targets were increased in *dcl1-fzt* mutants, including three MYB-domain transcription factors (miR159 targets), two ARF transcription factors (miR167 targets), three AP2-domain transcription factors (miR172e targets), and two F-box genes (miR394 targets) (Supplemental Table 4). In seedlings, 10 of 17 differentially expressed biologically defined targets were increased in *dcl1-fzt* mutants. Nearly all of the decreased seedling targets (6 of 7) are targeted by miR397, which targets laccases (Jones-Rhoades and Bartel, 2004; Zhang and Yuan, 2014). Decreased levels of multiple targets corresponding to a single miRNA raise the possibility that miR397 might have a positive role in gene expression, although miR397 downregulates its rice target, *OsLAC* (Zhang et al., 2013). Alternatively, another miRNA pathway could be epistatic to miR397 regulation, or the predicted miR397 targets might not be bona fide targets. Regardless, the differentially expressed high-confidence miRNA targets (based on mF $\leq$ 4 or functional conservation) were predominantly increased in *dcl1-fzt* plants. Although most mRNAs predicted to be miRNA targets were not differentially expressed in *dcl1-fzt* mutants, miRNA regulation often occurs only in a discrete group of cells at a specific developmental stage, and gene expression analysis at the tissue or whole-plant level is unlikely to uncover this regulation.

To verify our RNA-seq data, we examined the expression of 11 predicted target mRNAs and two pri-miRNA transcripts by quantitative RT-PCR (qRT-PCR) (Figure 6C). The quantitative PCR (qPCR) analysis gave similar results to the RNA-seq data, although in some cases the qRT-PCR analysis indicated a slightly larger fold change than the RNA-seq analysis. Regardless, there was strong agreement between the RNA-seq and qRT-PCR analyses.

DISCUSSION

fzt Contains a Mutation in *dcl1* and Is Defective in miRNA Processing

We identified a viable maize mutant in *dcl1*, the primary DICER enzyme involved in processing miRNAs in plants. To date, this is the only *dcl1* mutant reported in a plant other than *Arabidopsis*. Several pieces of evidence suggest that the *dcl1-fzt* allele results in decreased DCL1 function and that the *dcl1-fzt* phenotypes are due to decreased levels of a subset of miRNAs. First, *dcl1-fzt* behaves genetically as a partial loss-of-function allele; *dcl1-fzt* is completely recessive, and putative *dcl1* null alleles fail to complement *fzt*. Second, *dcl1-fzt* contains a mutation predicted to change a conserved serine residue in the RNase IIIa domain of DCL1. The RNase III domains contain the catalytic domains required for RNA cleavage of both the pri-miRNA and pre-miRNA (Kurihara and Watanabe, 2004; Zhang et al., 2004). Finally, miRNA levels are decreased and pri-miRNA levels are increased in *dcl1-fzt* mutants, consistent with reduced DCL1 function.

miRNAs were not uniformly reduced in *dcl1-fzt* plants. A few miRNAs (miR167a-d-5p and miR394a-b-5p) were dramatically reduced in *dcl1-fzt* mutants, others exhibit a moderate reduction, and another set were not reduced to a statistically significant level. The molecular basis for this differential effect on miRNA

Figure 5. (continued).

Differentially expressed miRNAs ($P < 0.05$) are indicated by black bars, and nonstatistically significant miRNAs are indicated by gray bars. miRNAs are listed in order of ascending P values. miRNAs decreased in both tissues are boldface and underlined. miRNAs that represent the miRNA* from the miRNA duplex are indicated with asterisks. Data shown are a summary of three biological replicates.

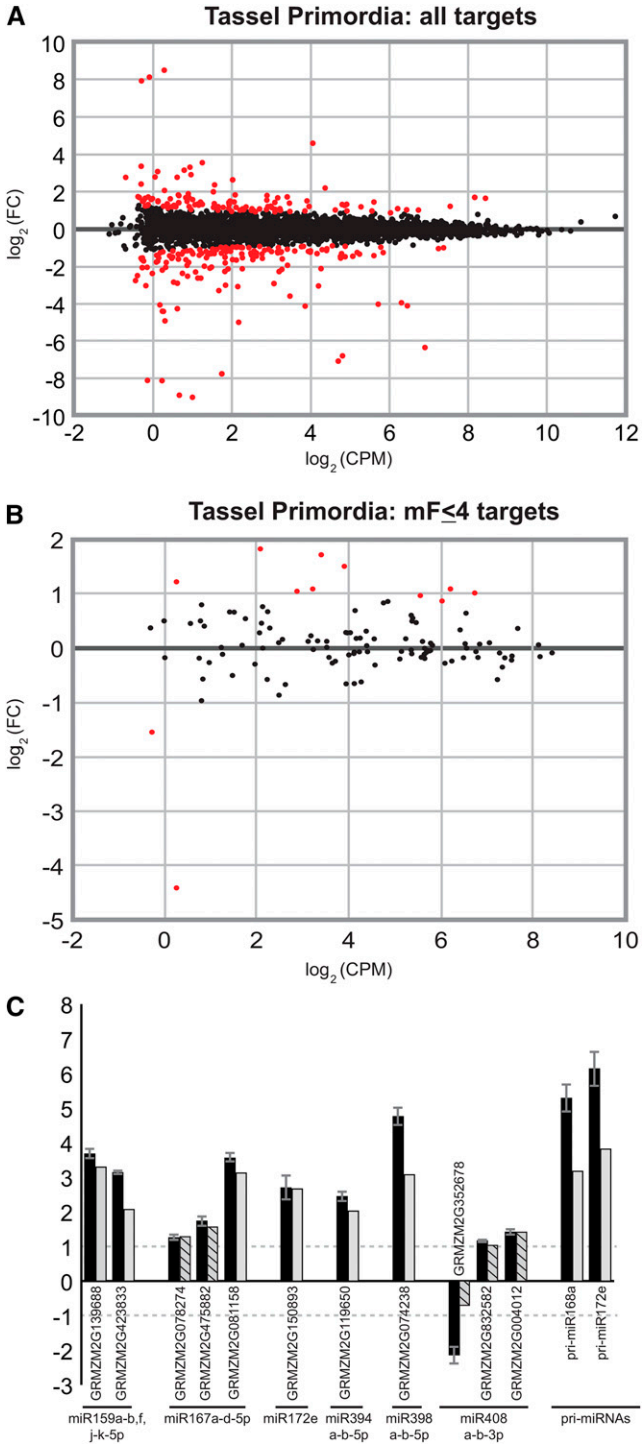

Figure 6. Analysis of Predicted miRNA Targets in Tassel Primordia.

(A) MA plot showing all predicted miRNA targets (mF ≤ 7) for miRNAs decreased in *dcl1-fzt* tassel primordia. Red dots indicate miRNA targets differentially expressed in *dcl1-fzt* mutants ($P < 0.05$ and FDR < 0.05), and black dots indicate miRNA targets that are not differentially expressed. miRNA targets are not broadly increased in *dcl1-fzt* mutants. CPM, counts per million; FC, fold change.

levels is unclear. One possibility is that the DCL1-FZT protein is defective in processing only a subset of pri-miRNAs with specific structural characteristics. Indeed, pri-miRNA processing seems to be particularly plastic in plants. Most plant pri-miRNAs are processed in a "base-to-loop" fashion by first cleaving the base of the hairpin and then a second cleavage 20 to 24 nucleotides from the initial cleavage site to excise the miRNA/miRNA* duplex (Cuperus et al., 2010; Mateos et al., 2010; Song et al., 2010; Werner et al., 2010). At least two miRNAs in *Arabidopsis*, miR159 and miR319, are processed in a more complex loop-to-base fashion that requires four cleavage events (Bologna et al., 2009). The processing mechanism of individual miRNAs has not been investigated in maize; thus, it is unclear if *fzt* mutants are defective in a particular processing pathway.

Alternatively, the differential effect on miRNA levels could be due to molecular redundancy, with DCL2 or DCL4 processing some miRNAs in the absence of fully functional DCL1. In *Arabidopsis*, DCL4 has been shown to process some miRNAs, including newly evolved miRNAs, with a high degree of complementarity within the pri-miRNA (Rajagopalan et al., 2006; Fahlgren et al., 2007; Ben Amor et al., 2009).

Maize *dcl1-fzt* mutants phenotypically resemble the *Arabidopsis dcl1* alleles *dcl1-9* (also known as *carpel factor* [*caf1*]) and *dcl1-100*, with reduced plant stature and leaf size, increased meristem indeterminacy, and meristem fasciation (Jacobsen et al., 1999; Laubinger et al., 2010). Although *Arabidopsis dcl1* alleles have similar effects on plant development, mutations in *dcl1* result in dramatically reduced miRNA processing and accumulation. Mature miRNA levels have not been globally examined in *dcl1-9/caf1* mutants; however, those miRNAs that have been examined are dramatically reduced or undetectable in the mutant (Park et al., 2002; Reinhart et al., 2002; Kasschau et al., 2003; Papp et al., 2003; Ronemus et al., 2006), and the pri-miRNA of at least some miRNAs accumulate in this mutant (Song et al., 2007). All miRNAs examined in the *dcl1-7* mutant allele are also similarly reduced or undetectable. Notably, the phenotype of *dcl1-7* is less severe than that of *dcl1-fzt*, and it produces some pollen (Robinson-Beers et al., 1992). *dcl1-100* mutants also exhibit increased levels of at least some, but not all, pri-miRNA precursors based on tiling array experiments (Laubinger et al., 2010). One unresolved question is why the *dcl1-fzt* mutation, with a more modest reduction in miRNA levels, exhibits severe phenotypes similar to *Arabidopsis dcl1* alleles. There is precedence that at least some single gene mutations have more dramatic consequences in maize than in *Arabidopsis*, particularly with regard to miRNAs. For example, *Cg1* has more severe phenotypes than *35S:miR156* in

(B) MA plot showing predicted miRNA targets with mF ≤ 4. Dot color indicates statistical significance as in **(A)**. Of the differentially expressed targets, the majority (12 of 14) are increased in *dcl1-fzt* tassel primordia.
(C) qRT-PCR validation of RNA-seq analysis for select miRNA targets and pri-miRNA transcripts. Black bars indicate fold change calculated from qRT-PCR analysis; gray bars indicate fold change calculated from RNA-seq analysis; gray cross-hatched bars indicate transcripts that do not meet the statistical threshold for differential expression in RNA-seq experiments. qRT-PCR data are the result of three biological and three technical replicates. Error bars indicate SE.

Arabidopsis (Wu and Poethig, 2006; Chuck et al., 2007a), and *ts4* has more severe phenotypes than loss of single *miR172* genes in *Arabidopsis* (Chuck et al., 2007b; Wu et al., 2009; Yumul et al., 2013). It is possible that the gene networks regulated by miRNAs are more robust in *Arabidopsis* than in maize, such that in maize, reduction of only a handful of miRNAs leads to severe phenotypic consequences.

miRNAs Are Required Broadly during Inflorescence and Vegetative Development

The wide range of reproductive and vegetative defects observed in *dcl1-fzt* plants underscores the broad roles of miRNAs during development. Some aspects of the *dcl1-fzt* phenotype can be explained by known miRNA regulatory networks, such as the regulation of meristem determinacy by *ts4*/miR172e and the control of phase change by miR156/miR172 and leaf polarity by miR390 and miR166 (Juarez et al., 2004; Chuck et al., 2007a, 2007b). Indeed, miRNA levels in *dcl1-fzt* correspond well to the severity of specific phenotypes. For example, miR172e is reduced >25-fold in the tassel and *dcl1-fzt* plants have severe meristem determinacy defects, whereas miR156a-i-5p, miR156l-5p, and miR166 are not statistically decreased in *dcl1-fzt* mutants, and *dcl1-fzt* plants have very mild phase change and leaf polarity defects. Interestingly, *dcl1-fzt* plants exhibit only relatively modest reductions in most miRNAs and their targets, suggesting that misregulation of a few miRNA target genes underlies most of the *dcl1-fzt* phenotype. In *Arabidopsis*, reduced levels of just two miRNA targets, *SPL10* and *SPL11*, largely suppressed the embryonic lethality of *dcl1* null mutations, indicating that a large part of the *dcl1* embryonic lethality is due to the misregulation of just two targets (Nodine and Bartel, 2010). Thus, even though the levels of most miRNAs are unchanged in *dcl1-fzt* plants, misregulation of just a few miRNA targets can have large and pleiotropic defects.

The individual miRNAs and/or their miRNA targets that underlie several aspects of the *fzt* phenotype are still unknown, but the pleiotropic effect is consistent with multiple affected miRNAs and includes phenotypic effects on stem cell homeostasis, plant height, leaf size, and floral organ and stamen development. miRNAs that exhibit large decreases in *dcl1-fzt* mutants are good candidates for being responsible for these aspects of the phenotype. Among the miRNAs that are severely reduced in *dcl1-fzt* tassel primordia are miR159, miR167, and miR319 (Figure 6), which target MYB transcription factors, auxin response factors, and class II TCP transcription factors, respectively, in *Arabidopsis* and have roles in stamen, ovule, leaf, and petal development (Palatnik et al., 2003; Millar and Gubler, 2005; Wu et al., 2006; Nag et al., 2009; Rubio-Somoza and Weigel, 2013). Importantly, miR159, miR167, and miR319 target these same classes of transcription factors in maize (Zhang et al., 2009), and *dcl1-fzt* mutants are defective in processes regulated by these miRNAs, including stamen and ovule development. Intriguingly, three MYB transcription factors targeted by miR159 (GRMZM2G423833, GRMZM2G139688, and GRMZM2G050550) as well two ARF transcription factors targeted by miR167 (GRMZM2G081158 and GRMZM2G07375) are statistically increased in *dcl1-fzt* mutant tassels (Figure 6C; Supplemental Table 4), consistent with three mRNAs contributing the *dcl1-fzt* phenotype.

MiR394 is also dramatically reduced in *dcl1-fzt* seedlings (>50-fold) and tassel primordia (>15-fold). In *Arabidopsis*, miR394 targets the F-box gene *LEAF CURLING RESPONSIVENESS* and functions as a mobile signal to establish stem cell niche organization (Song et al., 2012; Knauer et al., 2013). In maize, miR394 is predicted to target the F-box genes GRMZM2G119650 and GRMZM2G064954, both of which are broadly expressed during maize development, including in inflorescences (Sekhon et al., 2011). Interestingly, the levels of both targets are moderately increased more than 1.5-fold in *dcl1-fzt* seedlings and tassel primordia compared with normal controls (Figure 6C; Supplemental Tables 4 and 5). It will be interesting to investigate the role of these genes and how they relate to the *dcl1-fzt* phenotype.

miRNA Regulatory Networks Differ between Inbred Backgrounds

While *dcl1-fzt* mutants have similar phenotypes in all three inbred backgrounds examined, such as reduced plant stature, reduced leaf size, leaf polarity, phase change, and inflorescence defects, the severity of many of these phenotypes differs depending on inbred background. For example, leaf polarity defects are more severe in the Mo17 inbred background than in A619, and inflorescence defects are more severe in the B73 and Mo17 inbred backgrounds than in A619. Also, phase change occurs approximately one leaf late in the A619 inbred but approximately one leaf early in the Mo17 inbred background. Since the molecular defect in DCL1 is the same in each inbred (all contain the *dcl1-fzt* mutation, which presumably has the same effect on miRNA processing), these phenotypic differences suggest that genes functioning upstream or downstream of miRNA regulatory networks differ in the three inbreds. The identification of these modifier loci could provide a way to find genes in miRNA regulatory networks not amenable to standard genetic approaches. Most mutant screens isolate strong loss-of-function or null alleles, for which pleiotropy or epistasis might make it difficult to uncover roles in some developmental processes. The natural alleles present at these modifier loci, however, are likely mild alleles that have subtle effects in an otherwise normal genetic background and might provide targets for breeding programs. Similar background differences have not been reported for *Arabidopsis dcl1* alleles; thus, work in maize is poised to identify modifiers of miRNA regulatory networks and elucidate how these networks vary in natural populations to regulate plant growth and development.

METHODS

Genetics and Phenotypic Characterization

fzt was generated by EMS mutagenesis in the maize (*Zea mays*) A619 mutant background. Mapping populations were generated by crossing *fzt* heterozygotes to the Mo17 and B73 inbreds and self-pollinating. Mutants from segregating populations were tested for linkage to simple sequence repeat markers that spanned the genome. *fzt* was localized to chromosome 1, bin 1, and flanking markers were defined. The interval was refined

using available markers from the IBM neighbors map and additional single-nucleotide polymorphism markers designed based on maize ESTs in the interval.

The coding region was sequenced from one candidate gene, *dcl1* in the *fzt* allele, which corresponds to gene model GRMZM2G040762. This gene model is incomplete and lacks the conserved DEXD helicase domain found at the N terminus of all DCL proteins. The maize B73 reference genome contains a gap just upstream of gene model GRMZM2G040762; therefore, unordered contigs were assembled from overlapping BACs, AC155424, AC191351, and AC191256, and an additional ~53-kb sequence upstream of GRMZM2G040762 was reconstructed. To identify the full-length *dcl1* coding sequence, the predicted protein from GRMZM2G040762 was aligned to the predicted rice (*Oryza sativa*) DCL1 protein (Os03g02970; 1883 amino acids), revealing that GRMZM2G040762 aligns well with amino acids 577 to 1881 (92% identity) (Supplemental Figure 3). To identify the corresponding maize genomic sequences, OsDCL1 amino acids 1 to 576 were BLAST searched in CoGe (Lyons and Freeling, 2008) against the maize genome. This strategy was used iteratively with smaller segments of the N terminus of OsDCL1 to identify maize sequences that align to the entire N terminus. Comparison of the predicted maize DCL1 protein with that from *Arabidopsis* suggests that a short 114-nucleotide sequence encoding 38 amino acids annotated as an intron in rice is part of an exon. The predicted full-length maize DCL1 protein exhibits 90 and 72% identity to rice and *Arabidopsis thaliana* proteins, and the N-terminal domain, which contains the conserved DEXD domain, exhibits 85 and 59% identity with rice and *Arabidopsis* proteins, respectively (Supplemental Figure 3). See Supplemental Figure 11 for the full genomic sequence.

An additional *dcl1* allele was generated by crossing EMS-mutagenized Mo17 pollen onto *fzt* heterozygotes. One individual failed to complement the original *fzt* mutation in the F1, and the *dcl* coding region in this individual was sequenced. The Mu-insertion sites in the TUSC alleles that failed to complement *fzt* were also defined. Phenotypic characterization was done using *fzt* mutant families that had been backcrossed a minimum of three times to A619, Mo17, and B73. Seedling tissue for RNA analysis was genotyped by sequencing the region spanning the *fzt* mutation.

Vasculature polarity was examined by making hand sections of fresh tissue and staining with 0.5% toluidine blue O stain for 1 min, washing twice with water, and mounting in 100% glycerol for visualization with an Olympus BX41 microscope using a dark field. Epidermal peels were done as described (Gallagher and Smith, 1999).

Scanning Electron Microscopy

Tissue for scanning electron microscopy analysis was dissected and either mounted directly for scanning electron microscopy under low-vacuum conditions on an FEI Quanta 200 Mark 1 scanning electron microscope at an accelerating voltage of 10 to 15 kV or fixed in FAA, critical point dried, sputter coated, and viewed under high vacuum on a Hitachi S-4700 device at an accelerating voltage of 2 kV.

Small RNA and RNA-seq Library Sequencing and Informatics Analyses

A619 and *dcl1-fzt* mutant seedlings were grown for RNA analysis by germinating seeds on wet paper towels, transplanting seedlings to soil, and growing at 26°C with 12 h of light in a Percival AR-41L3 growth chamber for 14 d. Whole seedlings were removed from soil, washed, and flash-frozen in liquid nitrogen. Tassel primordia (0.5 to 1 cm) from *dcl1-fzt* and normal siblings were harvested from ~4.5-week-old plants grown in the East Carolina Biology Greenhouse with 16 h of light (two biological replicates) or in the field at the Central Crops Research Station in Clayton, North Carolina (one biological replicate), and flash-frozen in liquid nitrogen.

Total RNA from the materials described above was isolated using Tri Reagent (Molecular Research Center). Small RNA libraries were constructed using the Illumina TruSeq Small RNA sample preparation kit RS-200-0012. RNA-seq libraries were constructed using the Illumina TruSeq RNA sample preparation kit RS-122-2001. Libraries were sequenced on an Illumina HiSeq2000 instrument at the Delaware Biotechnology Institute of the University of Delaware.

The small RNA-seq data were processed as described previously (Nobuta et al., 2010; McCormick et al., 2011). In brief, small RNA libraries were trimmed to remove adapter sequences, low-quality reads were filtered out, and remaining reads (18 to 34 nucleotides) were mapped to the maize genome (Maize Genome Project 5b.60 AGPv2 sequences; http://www.maizesequence.org). The genome-mapped unique reads and their counts were imported to the R statistical environment (R Core Team, 2012). Lowly expressed reads (<1 count per million in less than two samples) were filtered out, library sizes were reset, and normalization was performed using the edgeR (Robinson et al., 2010) package default Trimmed Mean of M values method. Differentially expressed reads (small RNAs) were identified using the Generalized Linear Model approach implemented in the edgeR package. To account for multiple testing, the Benjamini and Hochberg method for controlling FDR was applied with a threshold ($q \leq 0.05$) to determine significance (Robinson et al., 2010).

Maize miRNAs annotated in miRBase 21 (mirbase.org) were mapped to this list to identify miRNAs present in each tissue. The seedling A619_3 miRNA abundances appeared elevated compared with its replicates; however, the difference between this nonmutant and mutant sibling pair appeared to be biological, and thus both libraries were included in the analysis.

Raw RNA-seq libraries were processed using an in-house pipeline to trim adapter sequences and filter out low-quality reads. TopHat (Trapnell et al., 2009) was used to map reads to the maize genome (AGPv2 sequences; http://www.maizesequence.org). Genome-mapped reads were assembled, and a "merged" transcriptome assembly was generated using Cufflinks. Quantification of expression levels for genes and transcripts was done using Cuffquant, and count tables were exported using Cuffnorm. These count tables were imported to the R statistical environment (R Core Team, 2012), and reads with low expression were filtered out followed by resetting the library size and normalization by the edgeR default Trimmed Mean of M values method. Mutant versus nonmutant contrasts were used to calculate differential expression using the Generalized Linear Model approach implemented in edgeR. Adjustment for multiple testing was performed by Benjamini and Hochberg's method (Robinson et al., 2010) to control FDR, and a threshold ($q \leq 0.05$) was used to determine significance.

Genome-wide identification of miRNA targets was performed using the sPARTA package (Kakrana et al., 2015). Putative targets were predicted using sPARTA's built-in target prediction module mirFerno with "standard" scoring schema and score cutoff of ≤ 7. At the cost of sensitivity, targets with scores ≤ 4 were investigated to maintain specificity (Figure 6B; Supplemental Data Sets 3 and 4) (Fahlgren et al., 2007). High-confidence target lists based on conserved biological functions (Supplemental Tables 4 and 5) used PFAM identifiers to assign likely biological functions to predicted maize targets. High-confidence targets were selected based on the known functions of conserved miRNAs and their targets in other plant species (Chorostecki et al., 2012).

Gene Expression Analysis

The expression of select target genes was examined using reverse transcription combined with qPCR. Total RNA was extracted from three biological replicates of normal and *dcl1-fzt* tassel primordia (four tassel primordia per biological replicate) using Trizol according to the manufacturer's recommendations. RNA was DNase-treated (RNase-free

DNase set; Qiagen), purified using the RNeasy mini elute kit (Qiagen), and reverse transcribed using oligo(dT) primers (SuperScript III first-strand synthesis system; Invitrogen). cDNA equivalent to 25 ng of total RNA was used in a 20-μL PCR with the MyIQ mastermix (Bio-Rad) on a Bio-Rad CFX96 real-time system; data were processed in CFX Manager (Bio-Rad) and Excel. Data represent averages of three biological replicates and three qPCR technical replicates. All primer efficiencies were between 95 and 105%, and data were normalized against *gapdh* levels. Sequences of the primers used can be found in Supplemental Table 6.

Accession Numbers

The small RNA and RNA sequence data have been submitted to the National Center for Biotechnology Information's Gene Expression Omnibus with accession number GSE52879.

Supplemental Data

The following materials are available in the online version of this article.

Supplemental Figure 1. Additional Phenotypic Characterization of *fzt* Plants.

Supplemental Figure 2. *fzt* Phenotypes Introgressed into the B73 and Mo17 Inbreds.

Supplemental Figure 3. Genomic Structure of Maize *dcl1*.

Supplemental Figure 4. *dcl1* Alleles Are Transmitted in Mendelian Ratios.

Supplemental Figure 5. Inflorescence Meristems Are Fasciated in *dcl1-fzt* Inflorescences.

Supplemental Figure 6. *dcl1-fzt* Leaf Polarity Defects in the A619 Inbred Background.

Supplemental Figure 7. *dcl1-fzt* Plants Have Phase Change Defects.

Supplemental Figure 8. Distribution of Small RNAs in *dcl1-fzt* and Normal Control Plants.

Supplemental Figure 9. Pri-miRNA Levels Are Increased in *dcl1-fzt* Mutants.

Supplemental Figure 10. Analysis of Predicted miRNA Targets in Seedlings.

Supplemental Figure 11. Maize *dcl1* Genomic Sequence.

Supplemental Table 1. Summary Statistics of Sequence-by-Synthesis (SBS) Small RNA and RNA-seq Libraries Used in This Study.

Supplemental Table 2. Abundance of miRNAs in Seedling and Tassel Primordium Libraries.

Supplemental Table 3. Abundance of pri-miRNAs in Seedling and Tassel Primordium Libraries.

Supplemental Table 4. Summary of Predicted miRNA Targets Based on Conserved Biological Function in *dcl1-fzt* and Normal Tassel Primordia.

Supplemental Table 5. Summary of Predicted miRNA Targets Based on Conserved Biological Function in *dcl1-fzt* and Normal Seedlings.

Supplemental Table 6. Primers Used in This Study.

Supplemental Data Set 1. Summary of Predicted miRNA Targets and Fold Difference in *dcl1-fzt* and Normal Tassel Primordia.

Supplemental Data Set 2. Summary of Predicted miRNA Targets and Fold Difference in *dcl1-fzt* and Normal Seedlings.

Supplemental Data Set 3. Summary of Predicted miRNA Targets (mF $\leq$ 4) in *dcl1-fzt* and Normal Tassel Primordia.

Supplemental Data Set 4. Summary of Predicted miRNA Targets (mF $\leq$ 4) in *dcl1-fzt* and Normal Seedlings.

ACKNOWLEDGMENTS

We thank David Hantz, Julie Calfas, and Julie Marik for care of greenhouse plants and Cathy Herring and Jim Holland for field space and assistance at the Central Crops Research Station. We also thank Amanda Wright for providing technical assistance with epidermal peels. This work was supported by the National Science Foundation (Grant 0604923 to S.H., Grant 1051576 to B.C.M., and Grant 1148971 to B.E.T.) and the National Institutes of Health (National Research Service Award postdoctoral fellowship F32GM082002 to B.E.T.).

AUTHOR CONTRIBUTIONS

B.E.T., C.B., R.H., A.K., B.C.M., and S.H. designed research. B.E.T., C.B., R.H., Q.D., T.-F.L., and S.A.S. performed research. B.E.T., C.B., R.H., Q.D., and A.K. analyzed data. R.M. contributed mutant stocks. B.E.T. wrote the article with substantial input from R.H., B.C.M., and S.H.

Received September 29, 2014; revised October 27, 2014; accepted November 13, 2014; published December 2, 2014.

REFERENCES

Aichinger, E., Kornet, N., Friedrich, T., and Laux, T. (2012). Plant stem cell niches. Annu. Rev. Plant Biol. **63:** 615–636.

Ambrose, B.A., Lerner, D.R., Ciceri, P., Padilla, C.M., Yanofsky, M.F., and Schmidt, R.J. (2000). Molecular and genetic analyses of the silky1 gene reveal conservation in floral organ specification between eudicots and monocots. Mol. Cell **5:** 569–579.

Aukerman, M.J., and Sakai, H. (2003). Regulation of flowering time and floral organ identity by a microRNA and its APETALA2-like target genes. Plant Cell **15:** 2730–2741.

Bartel, D.P. (2004). MicroRNAs: Genomics, biogenesis, mechanism, and function. Cell **116:** 281–297.

Bartel, D.P. (2009). MicroRNAs: Target recognition and regulatory functions. Cell **136:** 215–233.

Ben Amor, B., et al. (2009). Novel long non-protein coding RNAs involved in Arabidopsis differentiation and stress responses. Genome Res. **19:** 57–69.

Bensen, R.J., Johal, G.S., Crane, V.C., Tossberg, J.T., Schnable, P.S., Meeley, R.B., and Briggs, S.P. (1995). Cloning and characterization of the maize An1 gene. Plant Cell **7:** 75–84.

Bologna, N.G., Mateos, J.L., Bresso, E.G., and Palatnik, J.F. (2009). A loop-to-base processing mechanism underlies the biogenesis of plant microRNAs miR319 and miR159. EMBO J. **28:** 3646–3656.

Brodersen, P., Sakvarelidze-Achard, L., Bruun-Rasmussen, M., Dunoyer, P., Yamamoto, Y.Y., Sieburth, L., and Voinnet, O. (2008). Widespread translational inhibition by plant miRNAs and siRNAs. Science **320:** 1185–1190.

Bushati, N., and Cohen, S.M. (2007). MicroRNA functions. Annu. Rev. Cell Dev. Biol. **23:** 175–205.

Calderon-Villalobos, L.I., Kuhnle, C., Dohmann, E.M., Li, H., Bevan, M., and Schwechheimer, C. (2005). The evolutionarily conserved

TOUGH protein is required for proper development of *Arabidopsis thaliana*. Plant Cell **17:** 2473–2485.

Chen, X. (2009). Small RNAs and their roles in plant development. Annu. Rev. Cell Dev. Biol. **25:** 21–44.

Chen, X., Liu, J., Cheng, Y., and Jia, D. (2002). HEN1 functions pleiotropically in Arabidopsis development and acts in C function in the flower. Development **129:** 1085–1094.

Chorostecki, U., Crosa, V.A., Lodeyro, A.F., Bologna, N.G., Martin, A.P., Carrillo, N., Schommer, C., and Palatnik, J.F. (2012). Identification of new microRNA-regulated genes by conserved targeting in plant species. Nucleic Acids Res. **40:** 8893–8904.

Chuck, G., Cigan, A.M., Saeteurn, K., and Hake, S. (2007a). The heterochronic maize mutant Corngrass1 results from overexpression of a tandem microRNA. Nat. Genet. **39:** 544–549.

Chuck, G., Meeley, R., and Hake, S. (2008). Floral meristem initiation and meristem cell fate are regulated by the maize AP2 genes ids1 and sid1. Development **135:** 3013–3019.

Chuck, G., Meeley, R., Irish, E., Sakai, H., and Hake, S. (2007b). The maize tasselseed4 microRNA controls sex determination and meristem cell fate by targeting Tasselseed6/indeterminate spikelet1. Nat. Genet. **39:** 1517–1521.

Chuck, G., Whipple, C., Jackson, D., and Hake, S. (2010). The maize SBP-box transcription factor encoded by tasselsheath4 regulates bract development and the establishment of meristem boundaries. Development **137:** 1243–1250.

Chuck, G.S., et al. (2011). Overexpression of the maize Corngrass1 microRNA prevents flowering, improves digestibility, and increases starch content of switchgrass. Proc. Natl. Acad. Sci. USA **108:** 17550–17555.

Clarke, J.H., Tack, D., Findlay, K., Van Montagu, M., and Van Lijsebettens, M. (1999). The SERRATE locus controls the formation of the early juvenile leaves and phase length in Arabidopsis. Plant J. **20:** 493–501.

Cuperus, J.T., Montgomery, T.A., Fahlgren, N., Burke, R.T., Townsend, T., Sullivan, C.M., and Carrington, J.C. (2010). Identification of MIR390a precursor processing-defective mutants in Arabidopsis by direct genome sequencing. Proc. Natl. Acad. Sci. USA **107:** 466–471.

Fahlgren, N., Howell, M.D., Kasschau, K.D., Chapman, E.J., Sullivan, C.M., Cumbie, J.S., Givan, S.A., Law, T.F., Grant, S.R., Dangl, J.L., and Carrington, J.C. (2007). High-throughput sequencing of Arabidopsis microRNAs: Evidence for frequent birth and death of MIRNA genes. PLoS ONE **2:** e219.

Gallagher, K., and Smith, L.G. (1999). discordia mutations specifically misorient asymmetric cell divisions during development of the maize leaf epidermis. Development **126:** 4623–4633.

Gregory, B.D., O'Malley, R.C., Lister, R., Urich, M.A., Tonti-Filippini, J., Chen, H., Millar, A.H., and Ecker, J.R. (2008). A link between RNA metabolism and silencing affecting Arabidopsis development. Dev. Cell **14:** 854–866.

Griffiths-Jones, S., Grocock, R.J., van Dongen, S., Bateman, A., and Enright, A.J. (2006). miRBase: MicroRNA sequences, targets and gene nomenclature. Nucleic Acids Res. **34:** D140–D144.

Hugouvieux, V., Kwak, J.M., and Schroeder, J.I. (2001). An mRNA cap binding protein, ABH1, modulates early abscisic acid signal transduction in Arabidopsis. Cell **106:** 477–487.

Jacobsen, S.E., Running, M.P., and Meyerowitz, E.M. (1999). Disruption of an RNA helicase/RNAse III gene in Arabidopsis causes unregulated cell division in floral meristems. Development **126:** 5231–5243.

Jones-Rhoades, M.W., and Bartel, D.P. (2004). Computational identification of plant microRNAs and their targets, including a stress-induced miRNA. Mol. Cell **14:** 787–799.

Juarez, M.T., Kui, J.S., Thomas, J., Heller, B.A., and Timmermans, M.C. (2004). MicroRNA-mediated repression of rolled leaf1 specifies maize leaf polarity. Nature **428:** 84–88.

Kakrana, A., Hammond, R., Patel, P., Nakano, M., and Meyers, B.C. (2015). sPARTA: a parallelized pipeline for integrated analysis of plant miRNA and cleaved mRNA data sets, including new miRNA target-identification software. Nucleic Acids Res. **42:** e139.

Kasschau, K.D., Xie, Z., Allen, E., Llave, C., Chapman, E.J., Krizan, K.A., and Carrington, J.C. (2003). P1/HC-Pro, a viral suppressor of RNA silencing, interferes with Arabidopsis development and miRNA unction. Dev. Cell **4:** 205–217.

Knauer, S., Holt, A.L., Rubio-Somoza, I., Tucker, E.J., Hinze, A., Pisch, M., Javelle, M., Timmermans, M.C., Tucker, M.R., and Laux, T. (2013). A protodermal miR394 signal defines a region of stem cell competence in the Arabidopsis shoot meristem. Dev. Cell **24:** 125–132.

Krol, J., Loedige, I., and Filipowicz, W. (2010). The widespread regulation of microRNA biogenesis, function and decay. Nat. Rev. Genet. **11:** 597–610.

Kurihara, Y., and Watanabe, Y. (2004). Arabidopsis micro-RNA biogenesis through Dicer-like 1 protein functions. Proc. Natl. Acad. Sci. USA **101:** 12753–12758.

Kurihara, Y., Takashi, Y., and Watanabe, Y. (2006). The interaction between DCL1 and HYL1 is important for efficient and precise processing of pri-miRNA in plant microRNA biogenesis. RNA **12:** 206–212.

Laubinger, S., Sachsenberg, T., Zeller, G., Busch, W., Lohmann, J.U., Rätsch, G., and Weigel, D. (2008). Dual roles of the nuclear cap-binding complex and SERRATE in pre-mRNA splicing and microRNA processing in *Arabidopsis thaliana*. Proc. Natl. Acad. Sci. USA **105:** 8795–8800.

Laubinger, S., Zeller, G., Henz, S.R., Buechel, S., Sachsenberg, T., Wang, J.W., Rätsch, G., and Weigel, D. (2010). Global effects of the small RNA biogenesis machinery on the *Arabidopsis thaliana* transcriptome. Proc. Natl. Acad. Sci. USA **107:** 17466–17473.

Lee, D.Y., and An, G. (2012). Two AP2 family genes, supernumerary bract (SNB) and Osindeterminate spikelet 1 (OsIDS1), synergistically control inflorescence architecture and floral meristem establishment in rice. Plant J. **69:** 445–461.

Li, S., et al. (2013). MicroRNAs inhibit the translation of target mRNAs on the endoplasmic reticulum in Arabidopsis. Cell **153:** 562–574.

Liu, B., Li, P., Li, X., Liu, C., Cao, S., Chu, C., and Cao, X. (2005). Loss of function of OsDCL1 affects microRNA accumulation and causes developmental defects in rice. Plant Physiol. **139:** 296–305.

Lu, C., and Fedoroff, N. (2000). A mutation in the *Arabidopsis HYL1* gene encoding a dsRNA binding protein affects responses to abscisic acid, auxin, and cytokinin. Plant Cell **12:** 2351–2366.

Lyons, E., and Freeling, M. (2008). How to usefully compare homologous plant genes and chromosomes as DNA sequences. Plant J. **53:** 661–673.

Mateos, J.L., Bologna, N.G., Chorostecki, U., and Palatnik, J.F. (2010). Identification of microRNA processing determinants by random mutagenesis of Arabidopsis MIR172a precursor. Curr. Biol. **20:** 49–54.

McConnell, J.R., Emery, J., Eshed, Y., Bao, N., Bowman, J., and Barton, M.K. (2001). Role of PHABULOSA and PHAVOLUTA in determining radial patterning in shoots. Nature **411:** 709–713.

McCormick, K.P., Willmann, M.R., and Meyers, B.C. (2011). Experimental design, preprocessing, normalization and differential expression analysis of small RNA sequencing experiments. Silence **2:** 2.

Millar, A.A., and Gubler, F. (2005). The *Arabidopsis* GAMYB-like genes, MYB33 and MYB65, are microRNA-regulated genes that redundantly facilitate anther development. Plant Cell **17:** 705–721.

Morris, E.R., Chevalier, D., and Walker, J.C. (2006). DAWDLE, a forkhead-associated domain gene, regulates multiple aspects of plant development. Plant Physiol. **141:** 932–941.

Nag, A., King, S., and Jack, T. (2009). miR319a targeting of TCP4 is critical for petal growth and development in Arabidopsis. Proc. Natl. Acad. Sci. USA **106:** 22534–22539.

Nobuta, K., McCormick, K., Nakano, M., and Meyers, B.C. (2010). Bioinformatics analysis of small RNAs in plants using next generation sequencing technologies. Methods Mol. Biol. **592:** 89–106.

Nodine, M.D., and Bartel, D.P. (2010). MicroRNAs prevent precocious gene expression and enable pattern formation during plant embryogenesis. Genes Dev. **24:** 2678–2692.

Palatnik, J.F., Allen, E., Wu, X., Schommer, C., Schwab, R., Carrington, J.C., and Weigel, D. (2003). Control of leaf morphogenesis by microRNAs. Nature **425:** 257–263.

Papp, I., Mette, M.F., Aufsatz, W., Daxinger, L., Schauer, S.E., Ray, A., van der Winden, J., Matzke, M., and Matzke, A.J. (2003). Evidence for nuclear processing of plant micro RNA and short interfering RNA precursors. Plant Physiol. **132:** 1382–1390.

Park, W., Li, J., Song, R., Messing, J., and Chen, X. (2002). CARPEL FACTORY, a Dicer homolog, and HEN1, a novel protein, act in microRNA metabolism in *Arabidopsis thaliana*. Curr. Biol. **12:** 1484–1495.

Pautler, M., Tanaka, W., Hirano, H.Y., and Jackson, D. (2013). Grass meristems. I. Shoot apical meristem maintenance, axillary meristem determinacy and the floral transition. Plant Cell Physiol. **54:** 302–312.

Poethig, R.S. (2013). Vegetative phase change and shoot maturation in plants. Curr. Top. Dev. Biol. **105:** 125–152.

Prigge, M.J., and Wagner, D.R. (2001). The *Arabidopsis* serrate gene encodes a zinc-finger protein required for normal shoot development. Plant Cell **13:** 1263–1279.

Qin, H., Chen, F., Huan, X., Machida, S., Song, J., and Yuan, Y.A. (2010). Structure of the *Arabidopsis thaliana* DCL4 DUF283 domain reveals a noncanonical double-stranded RNA-binding fold for protein-protein interaction. RNA **16:** 474–481.

R Core Team (2012). R: A Language and Environment for Statistical Computing. (Vienna, Austria: R Foundation for Statistical Computing).

Rajagopalan, R., Vaucheret, H., Trejo, J., and Bartel, D.P. (2006). A diverse and evolutionarily fluid set of microRNAs in *Arabidopsis thaliana*. Genes Dev. **20:** 3407–3425.

Reinhart, B.J., Weinstein, E.G., Rhoades, M.W., Bartel, B., and Bartel, D.P. (2002). MicroRNAs in plants. Genes Dev. **16:** 1616–1626.

Ren, G., Xie, M., Dou, Y., Zhang, S., Zhang, C., and Yu, B. (2012). Regulation of miRNA abundance by RNA binding protein TOUGH in Arabidopsis. Proc. Natl. Acad. Sci. USA **109:** 12817–12821.

Robinson, M.D., McCarthy, D.J., and Smyth, G.K. (2010). edgeR: A Bioconductor package for differential expression analysis of digital gene expression data. Bioinformatics **26:** 139–140.

Robinson-Beers, K., Pruitt, R.E., and Gasser, C.S. (1992). Ovule development in wild-type Arabidopsis and two female-sterile mutants. Plant Cell **4:** 1237–1249.

Ronemus, M., Vaughn, M.W., and Martienssen, R.A. (2006). MicroRNA-targeted and small interfering RNA-mediated mRNA degradation is regulated by argonaute, dicer, and RNA-dependent RNA polymerase in *Arabidopsis*. Plant Cell **18:** 1559–1574.

Rubio-Somoza, I., and Weigel, D. (2011). MicroRNA networks and developmental plasticity in plants. Trends Plant Sci. **16:** 258–264.

Rubio-Somoza, I., and Weigel, D. (2013). Coordination of flower maturation by a regulatory circuit of three microRNAs. PLoS Genet. **9:** e1003374.

Schauer, S.E., Jacobsen, S.E., Meinke, D.W., and Ray, A. (2002). DICER-LIKE1: blind men and elephants in Arabidopsis development. Trends Plant Sci. **7:** 487–491.

Sekhon, R.S., Lin, H., Childs, K.L., Hansey, C.N., Buell, C.R., de Leon, N., and Kaeppler, S.M. (2011). Genome-wide atlas of transcription during maize development. Plant J. **66:** 553–563.

Song, J.B., Huang, S.Q., Dalmay, T., and Yang, Z.M. (2012). Regulation of leaf morphology by microRNA394 and its target LEAF CURLING RESPONSIVENESS. Plant Cell Physiol. **53:** 1283–1294.

Song, L., Axtell, M.J., and Fedoroff, N.V. (2010). RNA secondary structural determinants of miRNA precursor processing in Arabidopsis. Curr. Biol. **20:** 37–41.

Song, L., Han, M.H., Lesicka, J., and Fedoroff, N. (2007). Arabidopsis primary microRNA processing proteins HYL1 and DCL1 define a nuclear body distinct from the Cajal body. Proc. Natl. Acad. Sci. USA **104:** 5437–5442.

Steeves, T.A., and Sussex, I.M. (1989). Patterns in Plant Development. (Cambridge, MA: Cambridge University Press).

Till, B.J., et al. (2004). Discovery of induced point mutations in maize genes by TILLING. BMC Plant Biol. **4:** 12.

Trapnell, C., Pachter, L., and Salzberg, S.L. (2009). TopHat: Discovering splice junctions with RNA-Seq. Bioinformatics **25:** 1105–1111.

Vaucheret, H., Vazquez, F., Crété, P., and Bartel, D.P. (2004). The action of ARGONAUTE1 in the miRNA pathway and its regulation by the miRNA pathway are crucial for plant development. Genes Dev. **18:** 1187–1197.

Vazquez, F., Gasciolli, V., Crété, P., and Vaucheret, H. (2004). The nuclear dsRNA binding protein HYL1 is required for microRNA accumulation and plant development, but not posttranscriptional transgene silencing. Curr. Biol. **14:** 346–351.

Voinnet, O. (2009). Origin, biogenesis, and activity of plant microRNAs. Cell **136:** 669–687.

Werner, S., Wollmann, H., Schneeberger, K., and Weigel, D. (2010). Structure determinants for accurate processing of miR172a in *Arabidopsis thaliana*. Curr. Biol. **20:** 42–48.

Wu, G., and Poethig, R.S. (2006). Temporal regulation of shoot development in Arabidopsis thaliana by miR156 and its target SPL3. Development **133:** 3539–3547.

Wu, G., Park, M.Y., Conway, S.R., Wang, J.W., Weigel, D., and Poethig, R.S. (2009). The sequential action of miR156 and miR172 regulates developmental timing in Arabidopsis. Cell **138:** 750–759.

Wu, M.F., Tian, Q., and Reed, J.W. (2006). Arabidopsis microRNA167 controls patterns of ARF6 and ARF8 expression, and regulates both female and male reproduction. Development **133:** 4211–4218.

Xie, Z., Allen, E., Fahlgren, N., Calamar, A., Givan, S.A., and Carrington, J.C. (2005). Expression of Arabidopsis MIRNA genes. Plant Physiol. **138:** 2145–2154.

Yang, L., Liu, Z., Lu, F., Dong, A., and Huang, H. (2006). SERRATE is a novel nuclear regulator in primary microRNA processing in Arabidopsis. Plant J. **47:** 841–850.

Yu, B., Bi, L., Zheng, B., Ji, L., Chevalier, D., Agarwal, M., Ramachandran, V., Li, W., Lagrange, T., Walker, J.C., and Chen, X. (2008). The FHA domain proteins DAWDLE in Arabidopsis and SNIP1 in humans act in small RNA biogenesis. Proc. Natl. Acad. Sci. USA **105:** 10073–10078.

Yu, B., Yang, Z., Li, J., Minakhina, S., Yang, M., Padgett, R.W., Steward, R., and Chen, X. (2005). Methylation as a crucial step in plant microRNA biogenesis. Science **307:** 932–935.

Yumul, R.E., Kim, Y.J., Liu, X., Wang, R., Ding, J., Xiao, L., and Chen, X. (2013). POWERDRESS and diversified expression of the MIR172 gene family bolster the floral stem cell network. PLoS Genet. **9:** e1003218.

Zhang, D., and Yuan, Z. (2014). Molecular control of grass inflorescence development. Annu. Rev. Plant Biol. **65:** 553–578.

Zhang, H., Kolb, F.A., Jaskiewicz, L., Westhof, E., and Filipowicz, W. (2004). Single processing center models for human Dicer and bacterial RNase III. Cell **118:** 57–68.

Zhang, L., Chia, J.M., Kumari, S., Stein, J.C., Liu, Z., Narechania, A., Maher, C.A., Guill, K., McMullen, M.D., and Ware, D. (2009). A genome-wide characterization of microRNA genes in maize. PLoS Genet. **5:** e1000716.

Zhang, Y.-C., et al. (2013). Overexpression of microRNA OsmiR397 improves rice yield by increasing grain size and promoting panicle branching. Nat. Biotechnol. **31:** 848–852.

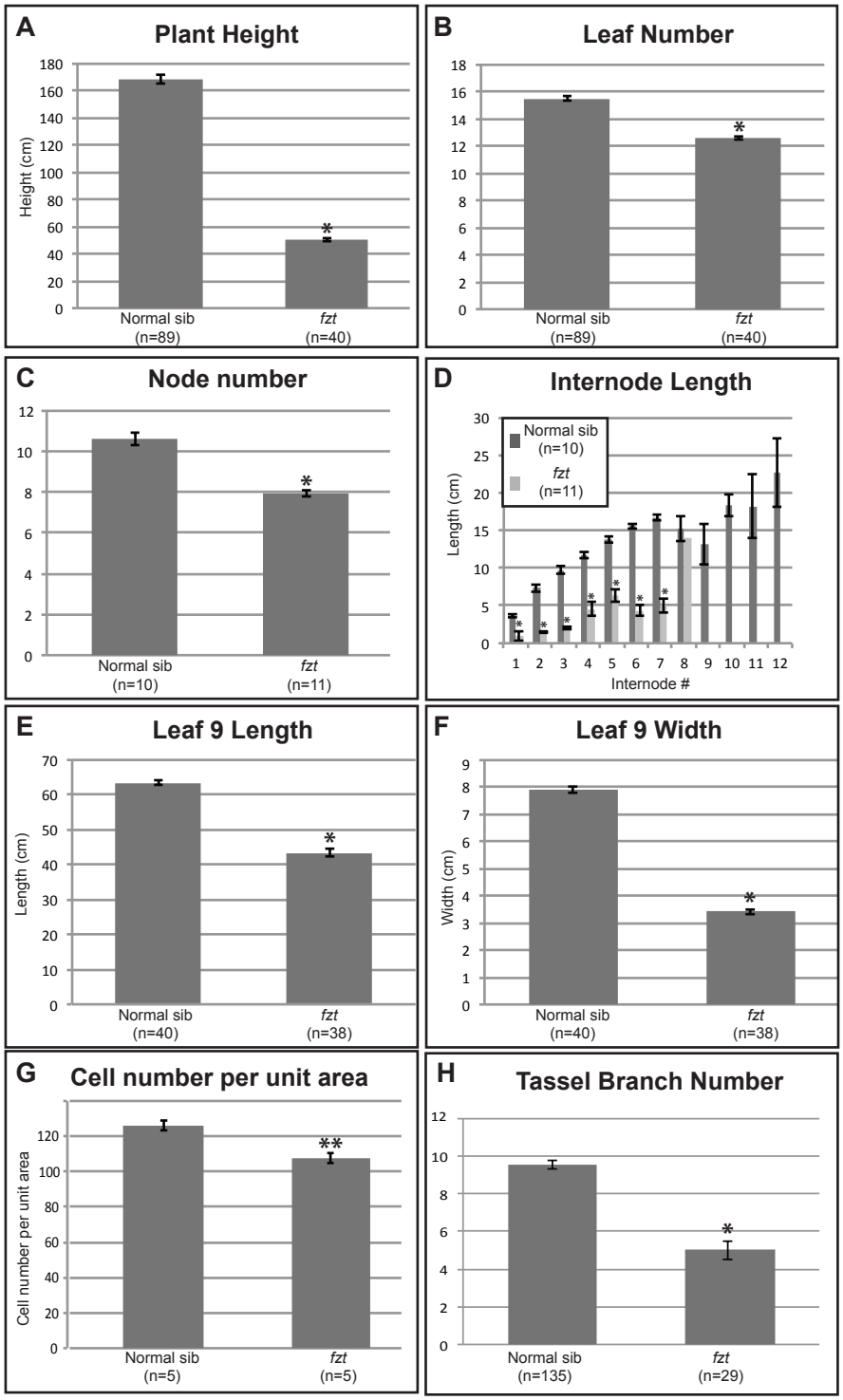

Supplmental Figure 1. Additional phenotypic characterization of *fzt* plants.
(A) *fzt* plants are shorter than normal siblings. **(B)** *fzt* plants make fewer leaves than normal siblings. **(C)** *fzt* plants have fewer nodes than normal siblings. **(D)** Internode length is reduced in *fzt* plants compared to normal siblings. *fzt* plants have shorter **(E)** and narrower **(F)** leaves than normal siblings. **(G)** Cell number/unit area in *fzt* and normal leaves. Cell number/unit area was slightly reduced in *fzt* and normal leaves, indicating that cell size is slightly increased in *fzt* compared to normal leaves. Leaf samples were taken from the middle of the blade of leaf 9. **(H)** *fzt* plants make fewer tassel branches than normal siblings. Data for **(A), (B)**, **(E)**, **(F)** and **(H)** are from field grown plants; data for **(C)**, **(D)**, and **(G)** are from greenhouse grown plants. Error bars indicate standard error. ** indicates $p < 0.05$ and * indicates $p < 0.01$ in a 2-tailed student t-test.

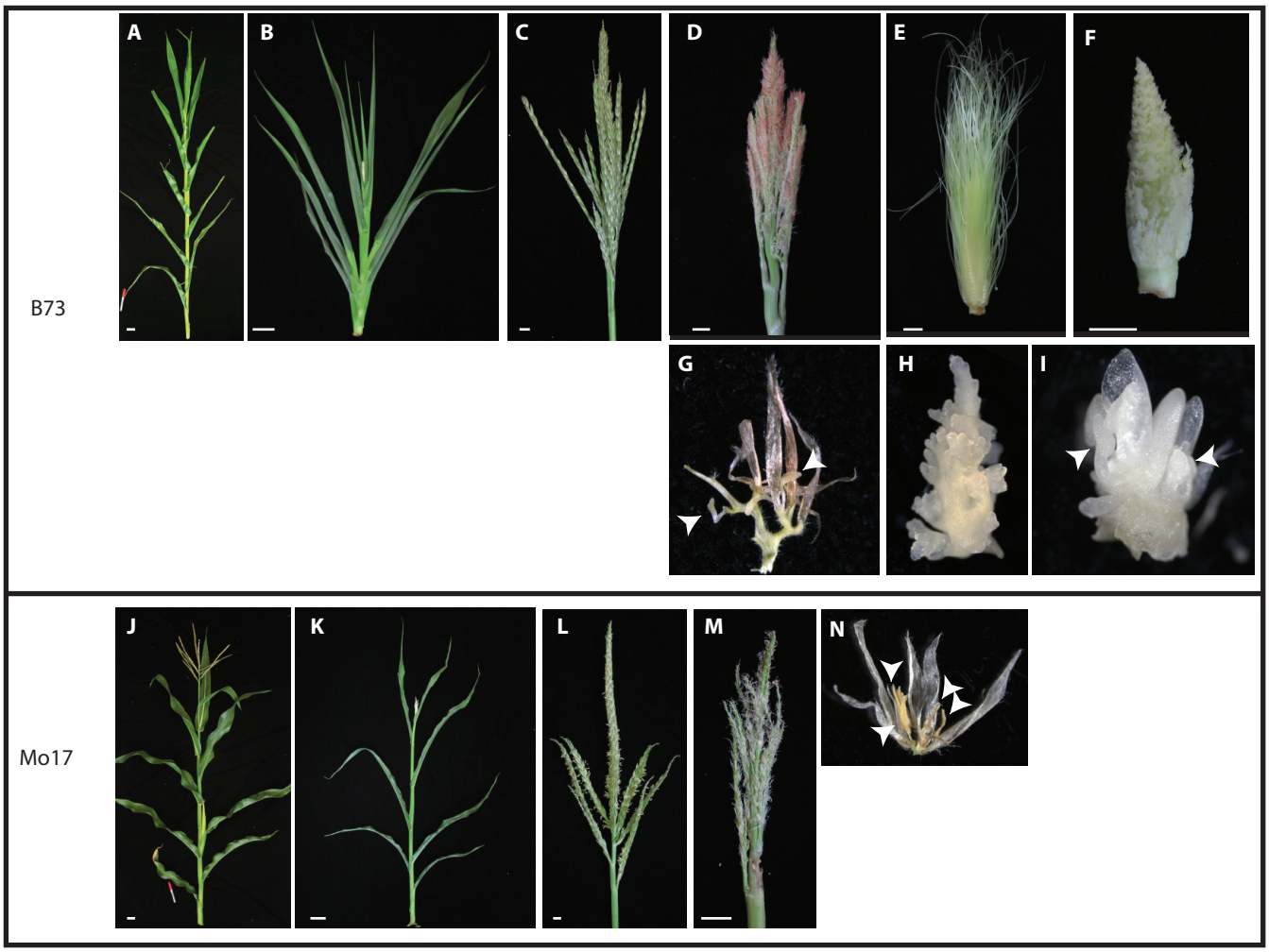

Supplemental Figure 2. *fzt* phenotypes introgressed into the B73 and Mo17 inbreds. **(A-I)** *fzt* and normal control plants introgressed into the B73 inbred background (5x) and **(J-N)** *fzt* and normal control plants introgressed into the Mo17 inbred background (5x). Normal plants **(A)** are much taller than *fzt* [B73] mutants **(B)**. Normal tassel **(C)** compared to *fzt* [B73] tassel **(D)**. *fzt* [B73] tassels are smaller than normal controls and are highly branched. Normal ear **(E)** compared to *fzt* [B73] ear **(F)**. *fzt* [B73] ears are highly branched and contain few floral organs. *fzt* [B73] tassel "spikelets" **(G)** contain an excess of palea/lemma-like organs and a few immature and abnormal stamens (arrowheads). **(H)** Branch from ear in **(F)** initiates meristems in a disordered manner. **(I)** Spikelet from ear in **(F)** contains immature stamens (arrowheads). Normal plants **(J)** are much taller than *fzt* [Mo17] mutants **(K)**. Normal tassel **(L)** compared to *fzt* [Mo17] tassel **(M)**. *fzt* [Mo17] tassels are smaller than normal controls and are highly branched. *fzt* [Mo17] tassel spikelets **(N)** contain lemma/palea-like organs and immature and abnormal stamens (arrowheads). *fzt* [Mo17] plants rarely make ears. Scale bars: A-B, J-K = 5cm; C-E, L-M = 1cm; F = 0.5cm.

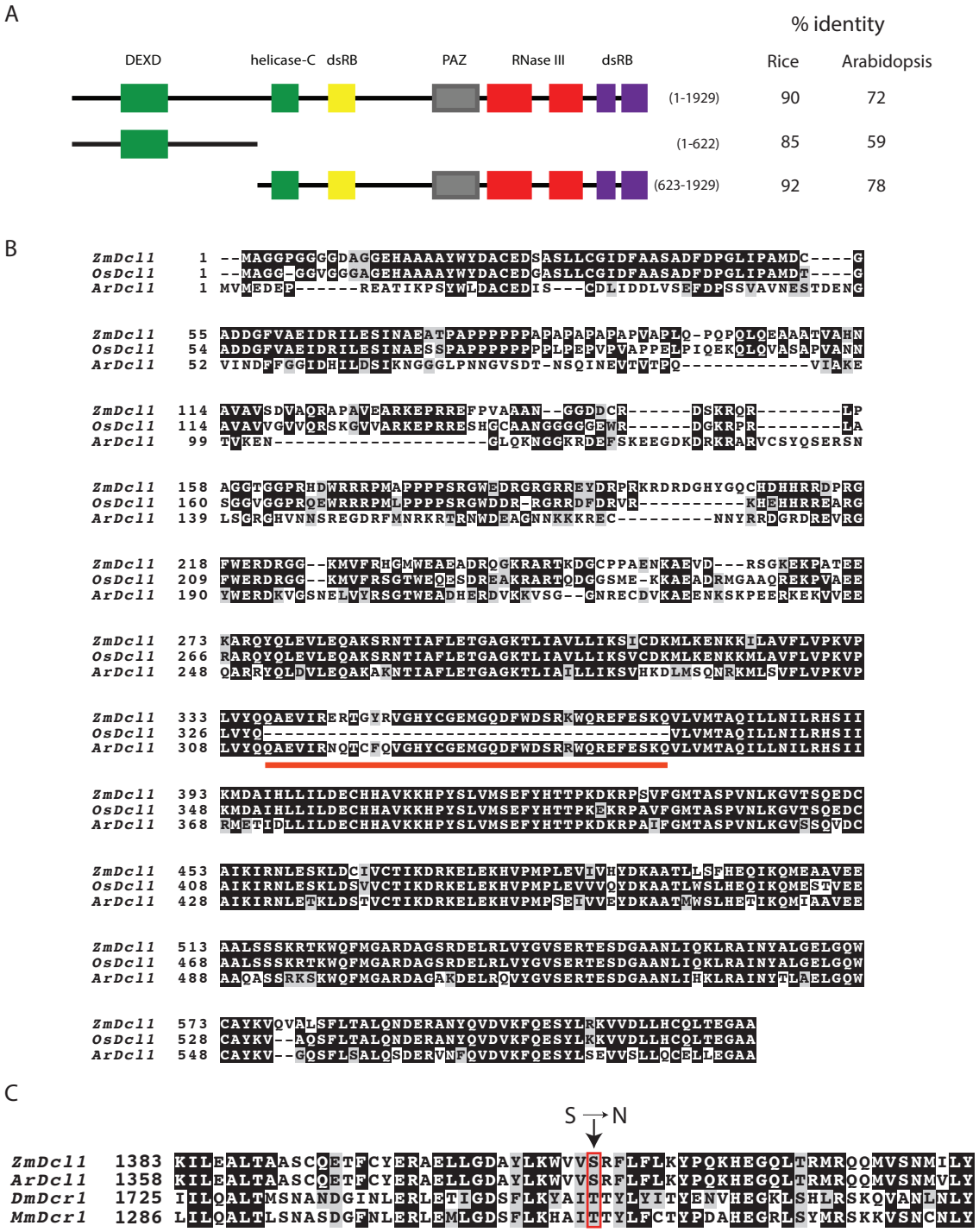

Supplemental Figure 3. Genomic structure of maize *dcl1*.
(A) The predicted maize full-length DCL1 protein is 1929 amino acids and contains a two part helicase domain (green boxes), a novel double stranded RNA-binding domain (yellow), PAZ domain (gray), two RNase III domains (red) and two C-terminal double stranded RNA binding domains (purple). The gene model GRMZM2G040762 corresponds to amino acids 623-1929 and lacks the conserved DEXD helicase domain at the N-terminus. The N-terminus of ZmDCL1 was predicted based on similarity to ArDCL1 and OsDCL1. Percent amino acid identity of ZmDCL1 to rice and Arabidopsis DCL1 full-length and partial proteins is indicated. **(B)** Amino acid alignment of the predicted N-terminus of ZmDCL1 (aa 1-622) to OsDCL1 and ArDCL1 is indicated. The red underlined amino acids are annotated as intronic sequences in rice, but exonic sequences in Arabidopsis. The high degree of conservation between Arabidopsis and maize suggest this sequence is exonic in both Arabidopsis and maize. **(C)** Alignment of part of the RNase IIIa domain, with the *fzt* mutation indicated. Alignments were performed using ClustalW2 (http://www.ebi.ac.uk/Tools/msa/clustalw2/) and shaded with BOXSHADE 3.21 (http://www.ch.embnet.org/software/BOX_form.html).

A

	Normal (%)	*fzt* (%)
dcl1-fzt/+ ⊗ (n=260)	201 (77.3%)	59 (22.7%)

B

	+ embryo (%)	- embryo (%)
dcl1-mum3/+ ⊗ n=172	123 (71.5%)	49 (28.4%)

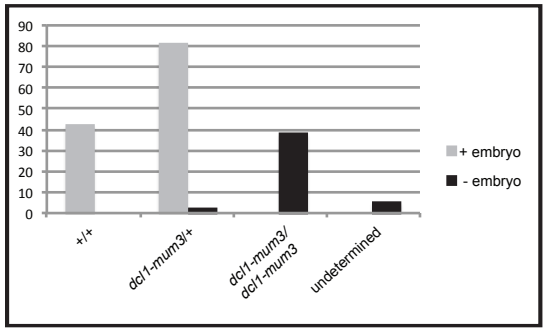

C

	+ / + (%)	*dcl1-mum3* / + (%)	und. (%)
dcl1-mum3 /+ x +/+ n=40	14 (35%)	25 (62.5%)	1 (2.5%)
+/+ x *dcl1-mum3 /+* n=42	20 (47.6%)	21 (50%)	1 (2.4%)

Supplmental Figure 4. *dcl1* alleles are transmitted in Mendelian ratios **(A)** One quarter of *dcl1-fzt/+* self progeny are *dcl1-fzt* homozygotes. **(B)** *dcl1-mum-3* homozygous seeds lack a recognizable embryo. Seeds were allowed to germinate on wet paper towels and embryos dissected for genotyping. For seeds that lacked an embryo, the whole seed including the endosperm was genotyped. **(C)** *dcl1-mum3* is transmitted normally through both the male and female gametophyte in reciprocal crosses. The genotypes of a few seeds were undetermined (und.) due to PCR failure.

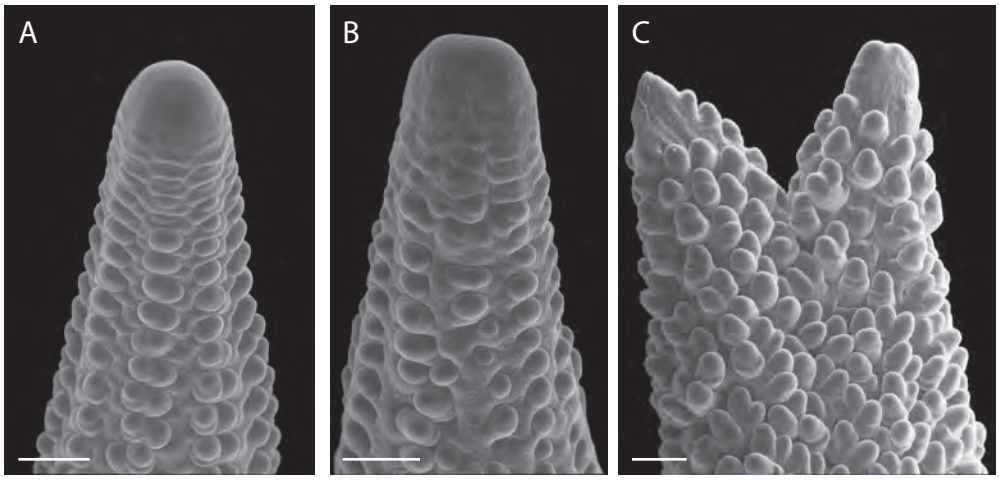

Supplemental Figure 5. Inflorescence meristems are fasciated in *dcl1-fzt* mutants.
(A) IM from normal ear forms a dome shape and grows as a single apex. **(B)** IM from young *dcl1-fzt* ear is broader and flatter than normal, indicative of mild fasciation. **(C)** IM from older *dcl1-fzt* ear has split into two apices, indicative of severe fasciation. Scale bars = 250μm.

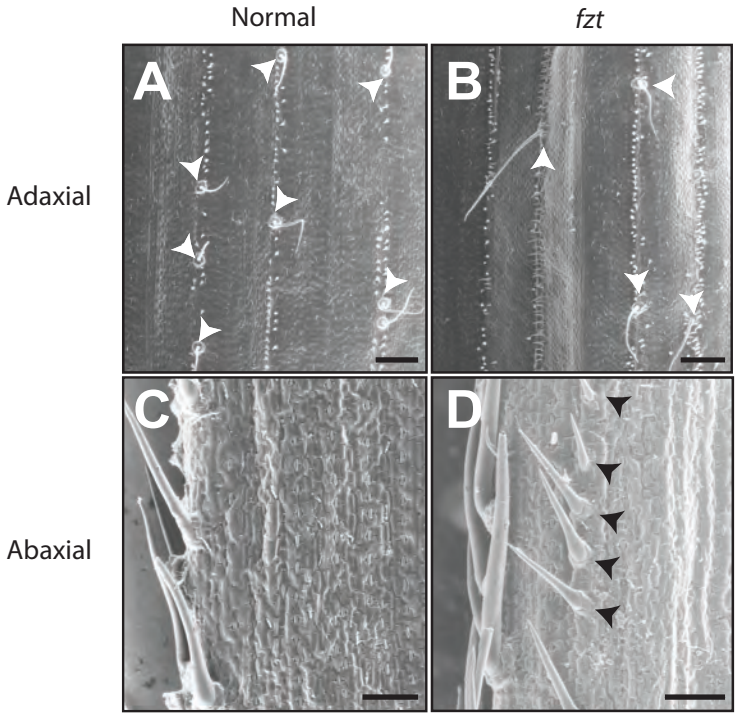

Supplemental Figure 6. *dcl1-fzt* leaf polarity defects in the A619 inbred. In normal leaves, macrohairs (arrowheads) are present on the adaxial blade **(A)**, but not on the abaxial blade **(C)**. In *dcl1-fz*t [A619] leaves, fewer macrohairs are present on the adaxial blade **(B)**, and extend onto the abaxial blade near the margin **(D)**. Arrowheads indicate macrohairs. Scale bars = 1mm A-B; 0.5 mm C-D.

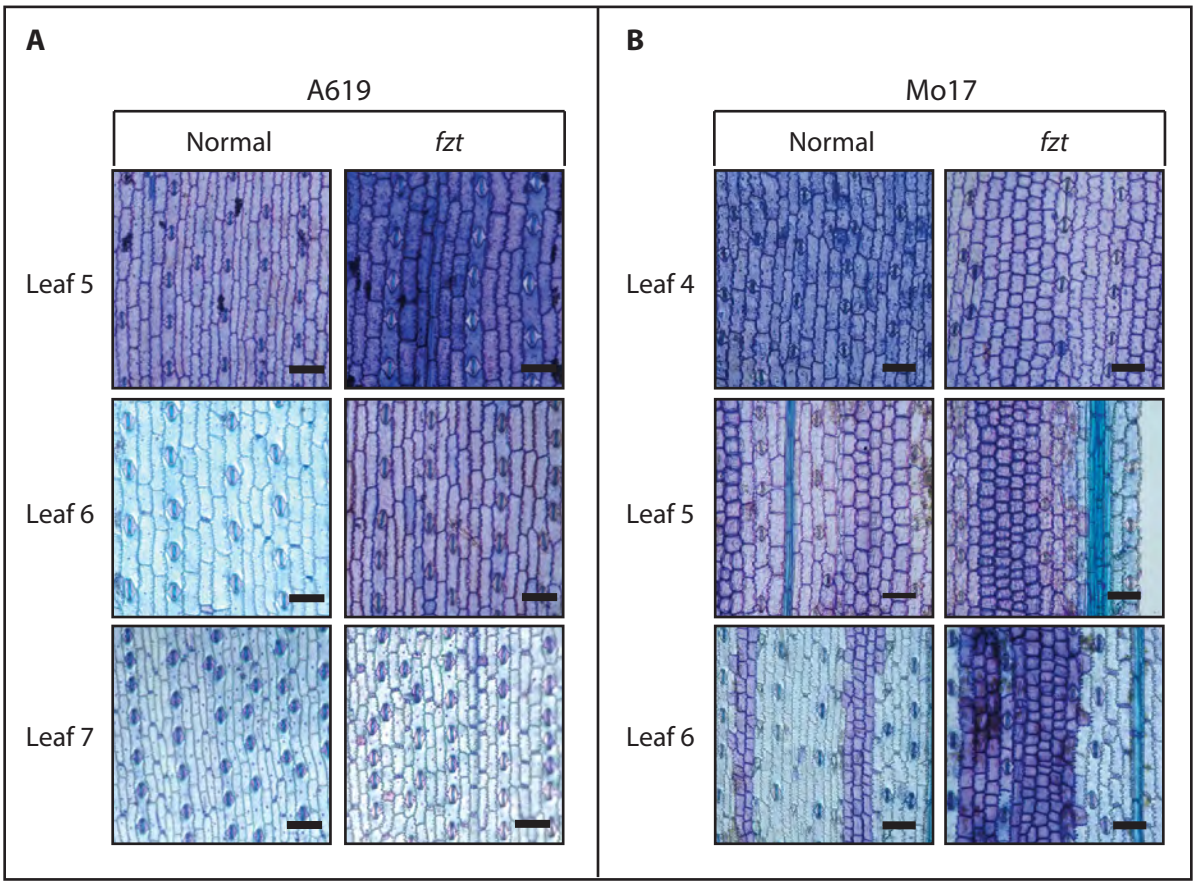

Supplemental Figure 7. *dcl1-fzt* plants have phase change defects.
(A) Toluidine Blue staining of epidermal peels from *dcl1-fzt* [A619] and normal leaves. Violet color indicates juvenile leaf waxes and light blue indicates adult waxes. *dcl1-fzt* [A619] plants transition to the adult phase ~1 leaf later than normal siblings. **(B)**Toluidine Blue staining of epidermal peels from *dcl1-fzt* [Mo17] and normal leaves. *dcl1-fzt* [Mo17] plants begin to transition ~1 leaf earlier than normal siblings. The violet stained cells in adult leaves are bulliform cells. Scale bars = 100 µm.

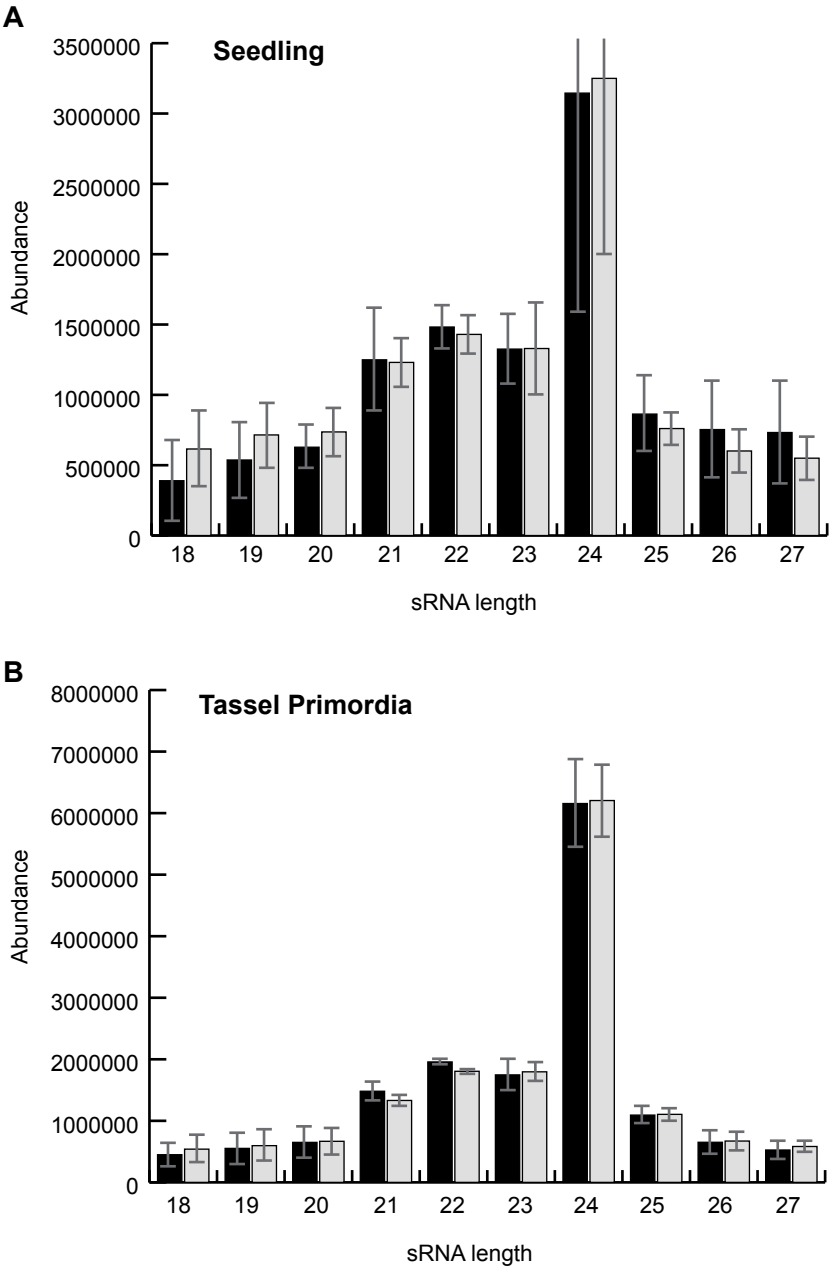

Supplemental Figure 8. Size distribution of small RNAs in *dcl1-fzt* and normal control plants.
(A) Size distribution of small RNAs in *dcl1-fzt* and A619 14 day old seedlings in three biological replicates. **(B)** Size distribution of small RNAs in *dcl1-fzt* and normal sibling control tassel primordia. There is no statistical difference in the abundance of 21-nt small RNAs, which are predominantly miRNAs, in *dcl1-fzt* and normal controls. Error bars indicate standard error.

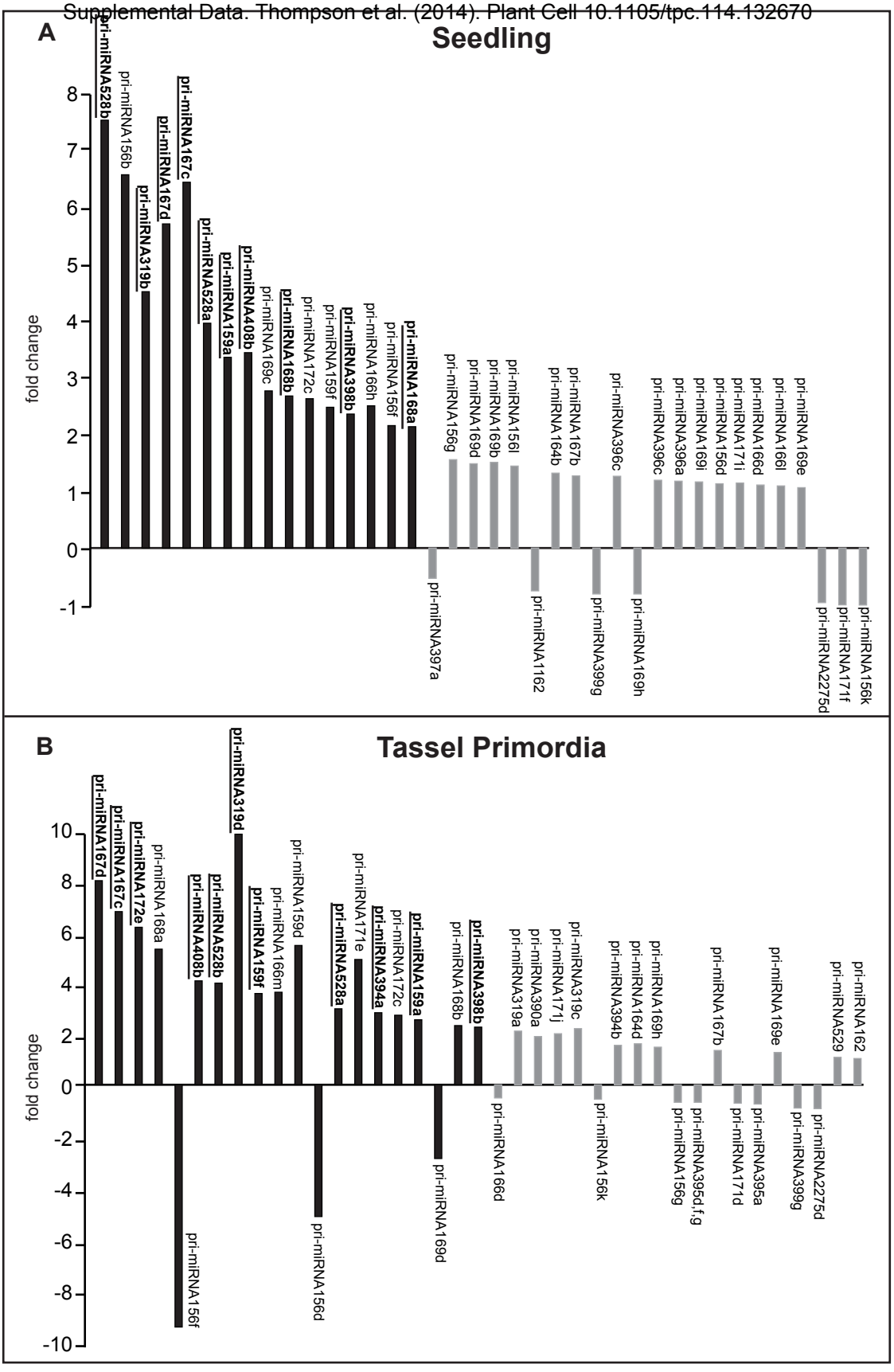

Supplemental Figure 9. Pri-miRNA levels are increased in *dcl1-fzt* mutants
(A) Comparison of individual pri-miRNA levels in *dcl1-fzt* and A619 seedlings.
(B) Comparison of individual pri-miRNA levels in *dcl1-fzt* and normal sibling tassel primordia. Differentially expressed pri-miRNAs ($p<0.05$) are indicated by black bars, non-statistically significant miRNAs are indicated by gray bars. Pri-miRNAs are listed in order of ascending p value. Pri-miRNAs for which the corresponding mature miRNA is decreased in *dcl1-fzt* are bolded and underlined. Data shown is a summary of three (tassel) or four (seedling) biological replicates.

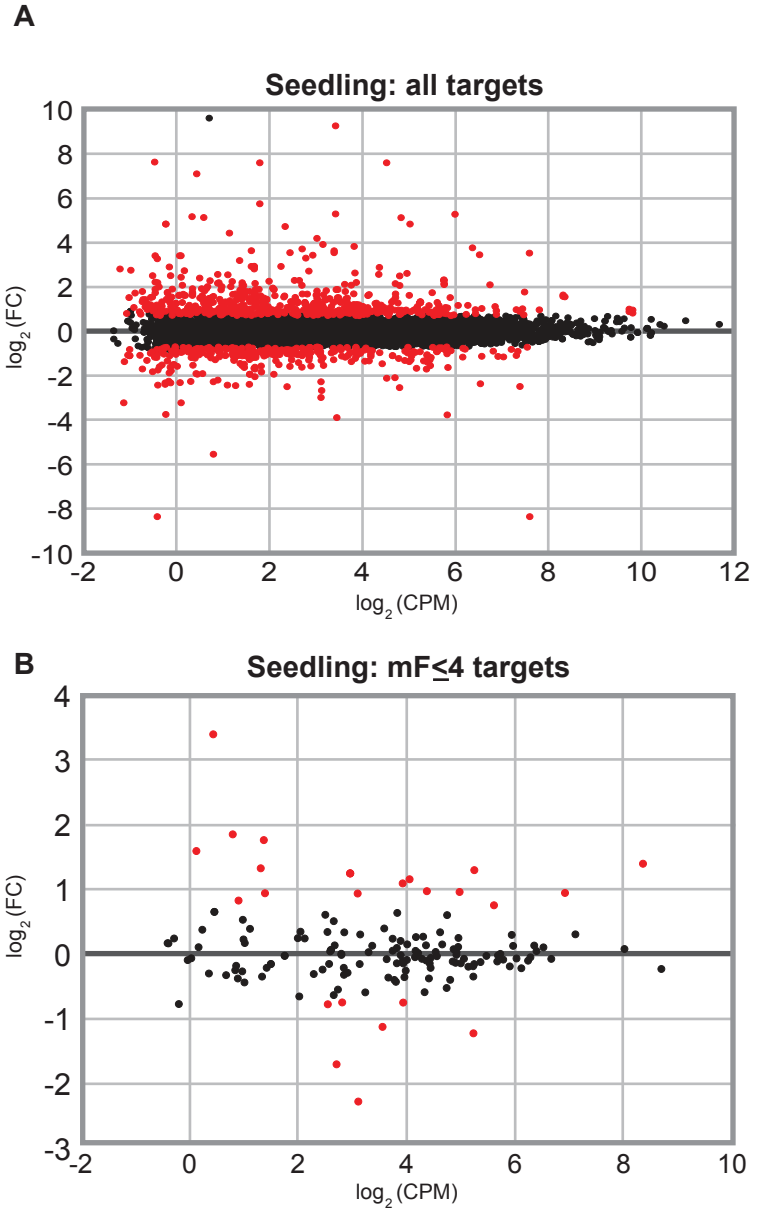

Supplemental Figure 10: Analysis of predicted miRNA targets in seedlings. **(A)** MA plot showing all predicted miRNA targets (mF ≤7) for miRNAs decreased in *dcl1-fzt* seedlings. Red dots indicate miRNA targets differentially expressed in *dcl1-fzt* mutants (p<0.05 and FDR<0.05) and black dots indicate mRNAs that are not differentially expressed. MiRNA targets are not broadly increased in *dcl1-fzt* mutants. **(B)** MA plot showing predicted miRNA targets with mF≤4 in seedling. Dot color indicates statistical significance as in **(A)**. Of the differentially expressed targets, the majority (19/26) are increased in *dcl1-fzt* seedlings. FC=fold change; CPM=counts per million.

Supplemental Figure 11. Maize *dcl1* genomic sequence
Reconstructed genomic sequence of *dcl1*-containing region (from BACs. AC155424, AC191351 and AC191256). Exon sequences are in highlighted in yellow. START and STOP codons are highlighted in red. We are coordinating with MaizeGDB to update the B73 reference genome (http://curation.maizegdb.org/curation/cgi-bin/displaylocusrecord.cgi?id=974366).

CATATTATTCAATGAGAATAAAATCCCATCAAACTCTTGCTGAAAATGACCTAAGTACACAA
TGTTTGGTGTTAGTCTATCGGTAGAAGACTCACCTTATCTTAGTTCATATTTTAAACTCTATT
AGTTAAATATAAAACACATTTGGCACGCATATATACGCAAGCTCAGATGGAGCTGGCCCGC
GAGACACGTGATGGATCCCTGACCCTAGCTGGTGCCGTCTTAAAGGCAGAGCAACCATGAT
AGTAGTAATTCAGGATTCCCGGGGGCAGAGGATCCCCTGTCGGGGTGCCCATAAATATCTCT
TCGTACTCCACACGCTTTGACTGCTCTGCTCGTAGGAAAGGCAAGGGCAGGCAGGGAGCGTT
CACTCCCATGGCACACTCCGTCTCCTGCAGGCAGTTCGCGGCTACGGACGGGCACTGACAGC
GCGCGCGCGGCCCACTCGGTGGTGGGTCGACCAGCCCGACACGCCCATGCCCGCACCGCAC
AGGGAGCCAGGGAGGAGTCATTCCACACGGCACGGTCCCCGCCACGGAGCTCGCGGCGGCA
CACGCCACCCGCACAGGCCCGCGCCGCTGCCGCTGGGCCCGCCAGGTCATTCCCGCACGACA
GGTAACAAATGCCCCAGTCCAAGGGCGGTTGGACCCGTACCGCACGAGCCCCGTGCTGGTG
CTGCAGTGCCTGGCTGCCTGCCCAGCATGCGTAGGGCGTGTAGCCCGCGCGCAGCCGCAATA
CCCCGCCCTAGGCCCGGTCCACCGCACCACACCCTGGAACCTGCACCCATGCCCCACACGTC
AGTGGGAGACAGACCGACCGACCTCTCCCCGTCTCACGGGTGCAGCCATTGGGGTGCCGGCT
CCGCTCGGCCCTCCTCTTCCTCGATTCGCAAGTCCCAACCCGCCTCTCCCACaAAGGCCAAAG
CCCCACCTGCTCCGTCGAGTCCCGTCGGCTCGCCCCGTCTCCCTCCCTCCTCcTcCCTCAAATC
ATATCATCAGAGCGAGAGGGACGGCGAGAGGAGAGCTGGGAAGGACagAGAGAGAGAGAG
AGTGAAGAGAAAGAGTAGCGTTGATACACCGTCGAATCGAATCGAGACCCTCCCTCCGCCC
CACCGCACCCCCCATATCGCATCGGAATCCAGCATCGCCATCGCCACCCCTCCATCGCACCA
CCGCTTTCCACTCTCCACTCCCTTCCCACCCTCGCCCCGCCCCGCCCCGCGCTTGCGTGATTC
GTACGGTTTATCACCGCCTCTTTCTCTTCCACTCTCTCTCCGTGGTTGGGTCCGGCTCGGTCCG
GTCCGGTCCGCCCGCCGCCGCCGCGGCACCCACTACAAGTAGTAGCGACATTCGTCTTCGCC
TCCTCTGCGATTCTTATTCTGATCCCCCGCCTCCCAAATGTGTTTTGCGCCTGCTGCCGCTGGT
TGAATACAGGAGGCGGGGCGTTGTTTGTTGTGGCCTGTAACTGTCGGCGTGGCAGCTGTTGG
TGCAGAGCGAGATGGCGGGAGGGCCAGGAGGAGGCGGCGACGCCGGCGGCGAGCACGCGG
CGGCGGCGTACTGGTACGACGCGTGCGAGGACAGCGCCTCCCTGCTCTGCGGCATCGACTTC
GCCGCGTCCGCCGACTTCGACCCGGGCCTCATACCGGCCATGGACTGCGGCGCCGATGACGG
CTTCGTCGCCGAGATCGACCGGATACTCGAGAGCATCAACGCCGAGGCCACCCCCGCACCG
CCGCCTCCTCCTCCTGCGCCTGCGCCTGCGCCAGCGCCAGCGCCTGTGGCTCCGCTGCAGCC
ACAGCCGCAGTTGCAGGAGGCGGCTGCGACCGTGGCCCACAATGCGGTGGCGGTGTCGGAC
GTGGCGCAGAGGGCCCCGGCCGTGGAAGCGAGGAAGGAGCCCAGGAGGGAGTTCCCGGTC
GCCGCGGCCAATGGCGGCGACGACTGCAGGGACAGCAAGCGCCAGCGTCTCCCTGCGGGTG
GTACCGGGGGACCACGCCACGACTGGCGGCGGCGTCCGATGGCGCCCCCGCCTCCATCCCGT
GGGTGGGAGGACCGGGGGCGCGGAAGGCGGGAGTACGACAGGCCTCGTAAGCGCGACCGC
GACGGCCACTACGGCCAATGCCATGATCACCACCGACGCGACCCTCGGGGTTTCTGGGAGC
GCGACCGCGGCGGCAAGATGGTGTTCCGCCATGGCATGTGGGAGGCTGAGGCGGACCGCCA
GGGAAAGCGTGCCAGGACGAAGGATGGATGCCCTCCTGCGGAGAATAAGGCGGAGGTGGA
TCGGTCGGGGAAGGAGAAGCCTGCCACTGAGGAGAAGGCGAGGCAGTACCAGCTCGAGGT
GCTTGAGCAAGCAAAGAGCAGGAACACAATTGCTTTCCTTGAAACTGGTGCGGGGAAGACT
CTCATAGCTGTGTTGCTCATCAAAAGCATCTGTGACAAAATGCTCAAGGAGAACAAGAAGA
TCCTTGCTGTCTTCTTGGTGCCTAAGGTGCCCCTTGTGTATCAGGTACAGACACACGAGTGAG
CCTTTGGACATTCAGGTCGCAAATTTTGTTGATACAATTATATTTTCTTGGTGGAATTGCAGC
AAGCTGAAGTGATACGCGAGAGGACCGGCTATCGTGTTGGGCACTACTGCGGGGAGATGGG
GCAGGATTTCTGGGATTCTAGAAAGTGGCAGCGCGAGTTTGAGTCAAAACAGGTAAAATCC

TGTGCGTGGCCGTACTTTTACTTCCAAACTATTTTCAGATACAATGCCCCATGGCCAAGCTTT
GATCAAACCTGTGCTTAGGCCACTTGAGTTAGGAACTATAGTGTAGTACTATGTTGTTGAGC
TAACTGGTTAGTAGCCGAGACACTTGCATTAAGTCTCATTGTTTCTTTGCAGATTATGAATTT
CTAAAAAAATTCTTTCTCTAGATGTAAACTAGTAGCCGAGGCACCTGCATTAAATCTGGCCG
TGCAGGACGTAAACTAGTTGGAGATCCAAATGCGTTGCACGCTCCAATTCCTAGCTTGGCAC
GGCGACACAGTACTCGGTAAAGGATCCAAGCATGCCCTTGGTTCCTCAGCTAGACTTGCCTC
AATGCCTCACCTCCTTACCTAGCCAAGGCTGGGGAGCCAAATTGTCTAGCCTGGGATAGCAA
TGAAAAACCTCGCCAACATAGAAAACGAGAGAGCTTGCCATCGATCGAAACACTCAACAGC
ATATGATTTCCTTGCCCAGTGAGGTGAGGCATGAGTTTCCCAAGGATCCAAACATGTCCCAG
GAATGGTTTTGATGGCACACTTTTGTGTGTTGAGAGGTGCATTGTGTTATTTGTTGTGTCTAA
CTGGAATTCTCATGGTCTTGGAATACTGGAATGCAATATGTTTAACTCATTCGTATCCcATAT
ATTCGTTCTTGCACCTAGCTTGTCTAACATGGTTTAAATGCACAAGCTGAAATATCTTGACTT
GCTAGAGCCGATAAGTGGTAAAAAAACTTCTTAGAAGATTGGGCTTAGGATAAGAAGGTAT
CCTATTTGCTTCCTGTTGTATTGTTAACCAGGAGGGATCATTACCACAATATTATATTCTGAC
TAAAATCCCAGTTTTTTAGAACTTTTGTCATTTTTCTCAACTTGTGGATTTAAGTGAGGGGGG
GGGGGGGGGATCCTTCGTGCTTATTTTCAGGATCATGGTAGATGTGTTTGTTGCCTTGAAAGT
CAACTAGGCACCTTTAGTATCACCATTTGCTTGCACTTAATCAGATGTATTGTGTAACACCCC
GTCCAATCCCTGGACCGGCAGTACTTACTCATGGCAGCTCTCTAGGATCATATATTGTCCCCA
CAGACCAACACGAGTCTTTTGTGCACACTTTGTCCTCACTCATGTGCACCCGAAAAAACTTC
CTAATCGGTCACCCATCCCAAATTGCTACAGGCCAAGCACGCTTAACTTAGGTTCTTTCGAG
ATAGGCTTCCGAAAAAGAAGATGCACCTTGTTGGTATGGATACCCTATTAATTCTATTAAGT
CTTGGGCCAGGAAATCACCATCCCAGGGACCAAGATATCACAATCCACCCCCCTTAGAAGA
CCGACGTCCTCGTCGGTCAACCCAAATCCAGGAACCTCCCCTCTTAGCCACGTCTGTGTGTTT
AGTGTCGTCATATGCCATACCATGTGACCACTCCGGGCCCACATGCGCAATGCGCTATATAC
CCGAACCCCCTAGCCCACACACGCCCGTGAAACCTTGAGGGTCGGCTCTGATACCACTTGTA
ACACCCCGTCCAATCCCTGGATCGGCGGTACTTACTCCTGGCAGCTCTCTAGGATCATATATT
GTCCCCACAGACCAACACGAGTCTTTTGTGCGCACTTTGTCCTCACTCATGTGCACCCGAGA
AAACTTCCCGGTCGGTCACCCATCCCGAATTGTTCCAAGTCAAGCATGCTTAACTTGGAGGT
TCTTTCGAGATAGGCTTCCGAAAAAGAAGATACACCTTGTTGGTACGGATACTCTTTTAATTC
TATTAAGCCCTGGGCCAGGAAATCACCATCCCAGGGCCAGTATATCACATATTGCAAGCAAA
ACAATTTGTTTTCTGTGTTATTGCTTCAGCAGGATGCTTGTTGTCTGTTACTTATCCATGTCTC
ACGCAGGTACTTGTTATGACAGCTCAAATTTTGTTGAACATCCTTAGGCACAGTATTATTAA
AATGGATGCCATACATCTTTTGATTTTAGATGAGTGCCATCATGCAGTGAAAAAGCACCCAT
ATTCTCTAGTAATGTCAGAATTCTATCACACCACTCCAAAGGACAAGAGACCATCTGTGTTT
GGCATGACTGCTTCACCTGTTAACCTGAAGGGTATGGCTCTCCTTAGTATATCCTTGTTATTC
CATGTACACTTTTCTTTGGCAGGTCCTGTCTCATTTAGATTTACTGCTCCTTTGCTTTCTGTTA
TATGTATGCTTTTCTGATGCTTAGTACTATATGGATAGGAGTGACTAGCCAAGAAGATTGTG
CTATCAAGATACGGAATCTTGAGAGTAAACTGGATTGCATAGTCTGTACGATCAAAGATCGG
AAAGAGCTGGAGAAACATGTTCCCATGCCTTTGGAAGTCATTGTCCACTACGACAAAGCAGC
CACTCTTTTATCTTTCCATGAACAAATCAAACAAATGGAGGCTGCAGTTGAAGAAGCTGCAC
TTTCTAGTTCTAAGAGAACTAAATGGCAGTTCATGGGAGCTAGAGATGCAGGGTCTAGAGAT
GAGCTACGTCTTGTCTATGGTGTTTCTGAGCGTACAGAAAGCGATGGTGCAGCTAATTTAAT
TCAGAAGTTGAGAGCTATAAACTATGCTCTGGGTGAACTAGGACAGTGGTGTGCTTACAAGG
TACTGCTTCACATCAGTGAACTAGTGTATTGATATCTGTTTCGTGTTTCTAACTGCTATATCT
GTTTAACTTCAGGTTGCACTGTCATTCTTGACAGCACTACAGAATGATGAAAGGGCCAACTA
TCAGGTTGATGTTAAGTTTCAAGAGTCATACTTGAGAAAGGTAGTTGATTTGTTACACTGCC
AGTTGACTGAAGGGGCTGCAATGAAAAGTGACAGTAATGATGTTGAAATGCATAATTCTGA
AAACCCCAAGCCAAATGAACTTGAGGAGGGAGAGCTACCTGACAGTCATGGTATTAATAGT
CTTCTTGCAAAATGTGTTATATGGTGACCTTTTTCTTTTTAACATTCCCCAATGAATTTCCCTT
CTTCCTTCACTCTACAATTAGCACATATTGTGTTTATTTTTTGTCCTTTATTATACCTTAGGAT
ATACAATTAGCACCTATTTTGTTTTTTTTTGTTCTTTATTATACCTGAGGGTATCTCAGCCTCA

CTTTTAACGCTTTATGCTGTTATTTCCCACTAGCTGTTTCTGTAGGTGAACATGTAGATGAAG
TCATTGGTGCCGCAGTGGCCGATGGAAAAGTTACCCCAAGGGTGCAAGCTTTGATAAAAAT
ACTTCTCAAGTATCAGCACACTGAGGATTTTCGTGCTATCATATTTGTAGAGCGAGTGGTTAC
AGCATTAGTCCTCCCTAAGGTAGGGACTATGTTTTCAACATCTTAAGATCAATTACTTCTCAA
CCTTTTATGAATTCTCTGACCTGTTTCCCTTTCACGACGGCTTAGGTCTTTGCAGAACTTCCAT
CGTTGGGCTTTATACGGTGTGCAAGCTTGATAGGTCATAACAATAACCAGGAGATGCGGTCG
TGCCAAATGCAGGATACAATCACAAAATTTCGTGATGGCCGTGTATGTTTCTATTCATGACG
ATGACATGATTTAACATAGTGTTTGTTGTGGCACACACCTTTTATGGTTTAACTATGTTGTTA
GCTAGGCTTAACGATCTGCATTCAGTGGTTTTATGCAATCTACTAAATTCCATGATGTCCAAG
TATGTTTCTACTCATGACAGAATTCTACATTCATATTTTTTGTTCCAAGTACATGTCTGTTGTA
AGTTTAAAACTATGTTTAACTGTGTGCTGTGTATATTTACGATTAAAACAGATATGTCCATGT
ACATATCTGTTGTACGTTAGGTGTATATATTGGAGTTGATCTGTGCCTCACAGGGTTTTTAAG
GCGTCGCCTAGGCGTCCAGTCGCTTGGCTAAACCTAGCCGCCTTGCCCGCCTAGGGCGCCGC
CTAGGCGCTAAGGCACTCGGAGTGTTTGCTTGCTCGCCTAGGCGCCTTAAGAACACTGGTGC
CTCATACACCAGCTATAAAAAATCTCTGTTATGGGTTTGCAGGTTACACTGTTAGTTGCAACT
AGTGTTGCAGAGGAAGGACTTGATATTAGGCAGTGCAATGTTGTCATTCGCTTTGACCTTGC
AAAGACTGTTTTGGCCTACATTCAGTCTCGGGGTCGTGCTAGAAAGCCTGGATCTGACTACA
TATTGATGCTTGAAAGGTAATTATGTGTCACCAAAACTCTTGATACCGTTAAAATATACTCC
ATTTAAATCATCGACTTATATAAATTAATTCTGCCAGAGGAAATATGTCTCATGAAGCTTTCT
TGAGAAATGCTCGGAATAGTGAAGAGACATTGAGAAAAGAAGCTATTGAGAGAACTGATCT
CAGTCATCTCGATGGCACTTCTATGCTAAGCCCTGTTGATATATCACCTGATTCTATGTATCA
GGTTGAATCAACAGGTGCCGTTGTCAGTCTGAACTCTGCAGTTGGACTCGTACATTTTTACTG
CTCACAGCTGCCGAGTGACAGGTACATAACTTCTTGTGATTTGTTTGGTATACTAGCTCAATT
GATTTTGAAATCGCAGGCTCATCAGTAGTTTCCTCATTCCAGATACTCTATTCTTCGACCGGA
ATTTATTATGCAAAAGCATGAGAAACCAGGGGGTTCAACAGAATATTCTTSCAAACTTCAAC
TCCCTTGTAATGCCCCATTCGAGAAACTTGAAGGTCCTATATGCAGTTCAATACGCCTGGCC
CAACAAGTAATGACAGTTCACTGGAACAAAATATTATTTAGTTTTTTTTCCGTACATTTTATC
TATTAGTTTGAACTGTGACTGGTTCTTTTTGTGCAGGCTGTTTGTTTAGCTGCTTGTAAGAAG
CTACATGAGATGGGTGCCTTCACAGATATGCTTTTACCTGACAGAGGAAGTGGGGAAGGAG
AAAAGACTGAACAAAATGATGAAGGTGATCCACTGCCTGGAACAGCACGCCATAGAGAGTT
CTTTCCTGAAGGGGTTGCTGAAATTCTACATGTCAGTATTTTCGTTCTCACATTACCTGAGCT
TGAACTTAACTTAATGGTGCTTTGCGAATTGCGATCTGCCGGTACTTTTAGGTTCTGATTAGT
TTCATTTCACTAAACTTTGTTTTCAACAGGGAGAATGGATTTTATCTGGAAGAGATGGTTACC
AAAGTTCACAGTTTATTAAGTTATATTTGTATTCTGTGAACTGTGTAAACATTGGGACTTCAA
AGGACCCTTTCGTTACACAACTTTCAAATTTTGCTCTTATTTTTGGCAATGAGCTGGATGCAG
AGGTAACTTTTTCCTGGTGATATTATGCAACTTGAGAAAATAAACATTTAAAATCCTATGAT
GTTTCGATGTTTTAGGTTTTATCGACGACGATGGATCTCTTTGTTGCTAGGACAATAATAACA
AAGGCATCTCTCGTATTCCGTGGACCAATTGAAATTACAGAAAGTCAGGTTAATTTTCTTTGC
AATGATGTATCAAAGTTCATTTCTATTTTTTACATTAAATGTTGCTAAACTTGCTCATGTGCTT
CCAGCTGATCCTGCTTAAGAGCTTTCATGTTAGGCTCATGAGCATTGTACTTGATGTTGATGT
TGATCCCTCAACAACTCCTTGGGATCCAGCAAAAGCATACCTCTTTGTTCCTGTGGGAGCTG
AGAAATGTATGGATCTTTTAAGAGAGATAGATTGGACTCTAGTTAATAGCATTGTGAATTCT
GATGCCTGGAACAACCCTCTTCAGAGGGCACGCCCAGATGTCTATCTAGGCACGAACGAAA
GGACACTTGGAGGGGATAGGAGGGAATATGGGTTCGGGAAGTTGCGCCATGGAACTGCATT
TGGACAGAAAGCCCACCCTACGTATGGTATCAGAGGAGCCATCGCTGAATTCGATGTTGTCA
AAGCGTCTGGATTAGTTCCTGGTCGTGGATGGGGACATTTTAATGATTATCAAAATAAAGGC
AAGTTGTTCATGGCAGATTCATGTTGGGATGCCAAAGATCTTGCTGGAATGGTTGTAACTGC
CGCCCACTCAGGAAAAAGGTTCTATGTGGACAGTATTTGCTATAATATGAATGCAGAAAATT
CTTTCCCTAGGAAAGAGGGCTATCTGGGTCCCTTGGAATACAGCTCGTTTGCTGATTACTAC
AAGCAGAAGTAAGATAAGTTTTGAGTGCTGGAAGCAAAAGGAGTTCTCTCTTAGCTCTACCT
CCTTTTGATTTCCCTTTTTTTTTGGCAAAGTAGCTTTATGGCAGCATACCATGATGATTCTTGT

TTTTCCTCTCAGGTATGGTGTGGAGTTAGTTTATAAGAAACAACCTCTTATACGGGCACGCG
GTGTTTCATACTGCAAAAATCTACTTTCTCCTAGATTTGAGCATTCTGAAGGTAAAAGCTATG
CATTTCTTTTGTGAGATTTCTTTTAGACTTTTTTTGTTTGCCTTAATATTTTGCTATTCATTGAT
GTTTTGGTCTTTCAAGCCCATCCAAGACTTCCCAGCACTAGATTAATTTAATAAAGAAATAC
AAACTTAGTGCTTAATATAACTTATATACTTGCAAATGGGAAAGTGTTTGGTATAATGGATT
TGTACTACTATTGTTTTGCAGCTAGCAATGGAGAGTTCTCAGAGAATCTTGACAAGACATAC
TATGTATATTTACCACCCGAATTGTGCCTTGTGCATCCTCTCCCCGGATCACTTGTTCGTGGA
GCTCAGAGGTTACCCTCAATAATGAGAAGGGTGGAGAGCATGCTTCTTGCAATTCAACTGAA
GGACATAATTGGGTATCCAGTTCCTGCAAATAAGGTACACTTGCAGCTCCCAATCGAGCATG
TTTTAGGGAAAACTTTTGAATGTCCCCCGGTAGAATTTACCGGTAAATTGAACACTTAAATTT
GTCCTTTCTATATTACACAACTGTCTTCTACTAAGATGTCAGACTACATGCCAACTAAGTGGA
GCACCCAATGACACCTCTAGGCCTTCATTGTTGCTCCTAGCCTTGGTGGATCGTGTCTGTTGA
CGGGAAAAAATTGTTAAACAAACCAATATGTACTCAATCCAGGTGCTACTGAATACTAATGA
TAGTTTTGTACATGATAATATGCAGGGTAAATTTAAGGGTCTAGTCTTCTGAAAAGATCATG
CTTGTTTGCCTAATGAAAAAAATGTGGAGTGCCATAAACCTGTTCTCTATTCACCTAGATTCA
TCATGCAATAGCTATATGTTATTCTGCACATTGATTAATAATTAATAGCTTTTTGTTTGTGTG
GTTCACAGATATTAGAAGCCTTGACTGCTGCGTCATGCCAGGAGACATTCTGCTATGAAAGA
GCAGAGCTGCTGGGTGATGCATACTTGAAATGGGTTGTGAGTAGATTCCTTTTCCTAAAATA
TCCTCAAAAGCATGAGGGACAGCTCACAAGGATGCGGCAGCAGATGGTTAGCAACATGATC
CTGTATCAATACGCCCTGAATAAAAACCTCCAATCTTATATCCAAGCAGATCGATTTGCTCC
ATCAAGATGGGCAGCTCCAGGAGTGTTACCTGTATTTGATGAAGAAACGAGAGATTCTGAA
CCATCCATCTTTGATGAGGAATTTACTCCTAGCAGTGAGTTACAAAAGAACTTGTATGATGA
CTATGATGGCGATAGCATGCAAGAAGACGGTGAAATTGAGGGAGATTCTAGCTGCTATCGT
GTTCTATCAAGCAAAACATTAGCAGATGTTGTGGAAGCACTTATTGGTGTCTATTATGTAGC
TGGAGGGAAAATTGCTACAAACCATCTGATGAAATGGATCGGTATTAATGCAGAGTTGGAT
CCTCAAGAGATCCCATCTTCGAAGCCATATAACATACCTGAGAGCATAATTAAAAGCATCAA
TTTTGACACATTAGAGGGTGCATTGGGTATCAAGTTTCAGAATAAAGGCTTACTTGTTGAAG
CTATAACACATGCATCAAGACCATCATCAGGTGTTTCCTGTTACCAGCGCCTGGAATTTGTTG
GTGATGCTGTATTGGACCATCTCATTACGAAGCACTTATTTTTTACTTATACGGACCTACCTC
CAGGCCGCTTGACTGACTTGAGAGCTGCAGCTGTTAATAATGAGAACTTTGCAAGGGTTGCA
GTTAAACATAAGCTACATGTACATCTTCGCCATGGATCATCTGCATTGGAGACACAGGTGGG
CCATTCTTAATGTTCAGTAGTGAACTTCCTTGCTACCCACTCCATTCCAAATTATTATTTTTAT
ATGCATAGCTTTTTATGCACTTAGAAATACATTATGTCTAGATTTGTAGTAAAAAACAGTGT
ATCTAGAAAAGCTAAAACGCCCTGTAATTTGAAATGAATGGAGTATGTGTTACTTATATATG
CTGTAATGTTTGAACTAGAGTTCTGTCATGTTGAAAATATTGGCACCTTTTGGAAGCAGTGCT
GACTATATTCTCTCTATCCTGTGAAGATTCGAGAGTTTGTGAAGGATGTCCAGGAGGAGCTT
TCGAAACCAGGTTTCAATTCTTTTGGCCTTGGGGATTGTAAGGCTCCAAAGGTTCTCGGAGA
CATTTTTGAGTCTATTGCTGGCGCAATATTCCTTGATAGTGGGTGTGCTACCTCCGTAGTCTG
GAAGGTAGTTTCTGTGTTCTTTGGAATGAAATTCTGTTCATACTCATGTGGGAAATACTGAA
GTTTAATTTTTTTAATCCATCATGTCAGGTTTTTCAGCCTCTGCTTGATCCAATGGTGACGCC
GGACACCCTTCCGATGCACCCTGTAAGGGAGCTCCAAGAGCGCTGCCAGCAGCAAGCCGAA
GGATTAGAATACAAAGCATCCCGTACAGGCAATGTAGCTACAGTTGAAGTCTTGGTTGATGG
CATACAGATTGGTGTAGCTCAGAACCCACAGAAGAAGATGGCACAAAAGTTGGCGGCTAGA
AATGCACTTGTTGTCTTGAAAGAGAAGGAAACCGCAGCAAAGAAAGACACTGAAAAGGATG
GCGAGAAGAAAAACGGTTCTCAGTTCACTAGGCAGACTCTGAACGACATCTGCTTGAGAAG
GCAATGGCCGATGCCACAGTACAGGTGTATAAACGAGGGTGGCCCTGCCCATGCCAAAAGA
TTTGTTTATGCGGTAAGGGTAAATACATCTGACAGTGGATGGACTGACGAGTGCATTGGAGA
GCCAATGCCGAGTGTGAAAAAGGCCAAGGACTCTGCAGCTGTTCTTCTGCTCGAGCTGCTGA
ATCGAAATTACCGTGGCAAGCCTGATGGAAAATAATCTTTGGTGATGTTCTGTGGTGGTAGG
TAGACGTGGAAGCATCCATCATTCTGATTATACCCCCATGCAGTGCTTTTCAGCAAAGCAAA
TTAATGGCCTTTGTTGATGTTCTTGGTGGCGGTATTGGTGATATGGAGGCATTCAATGCAAGC

ATAAGCAGAGCTATGGGGAGTGGGATTAGAGGATTATTATTAGTTTTGTCTGAGGTGACTAC
TAGGTATTTTACTGGCGAGGTACTGAGGTCACAACTCACAAATAGCAGTTGCAAATTGCAAT
AGAGGAAATGATGATAGGTTGATATAGGATATTGGAGGCCTCTTATTCATCGATTGTATAAG
ATGTTTACAGAACAGTGCATTGATCCATTAAATTTATATTGATTGATATTTTTATAGTGGTAT
ACTACTAACGGCTTTCTTATATTTCGTCCCGCTATGTATTCAGTGGCTTAGATGTTTACAAAC
ATCTCACATTCATACACAGGATGCGCCTGCAGCTGGGAACTCGGGGTTCTCTATCTTGGCCT
CGCCGACCAAATATCACGTACGTCGACGTCCGCGAACAGTATATATATGGTAGGCTTGGTAA
GGCTCCTTCCTTCGCACCAACCAATTAGTGACCTGGTTCATCAGCATAAACACACACGTTAC
TCACCTTTCGCATGGACCACTCAGTTTGTCACTGAAAATACTTGTAGGCGGGCGTGATCCCCT
TGCGCATGGTACAGAGCAAGACGCTGAGCTGGATATTCTGATAATCCCGTATACTCCAACAG
AAACTACAGAATGGAATCAAGTTGTACCTGCGTTTCTGCTGCTCAAAAATTGCGAGATGGAC
CATGGACGTGTGTTGTTTGGCAACAACGACGCAACCAGCACGGACAAGAAGGGGGGACATG
CAGTCTCTCGAAACCTGTCCTATACAATTAGAAAGAAAAAAAAGAGGGAAAATAAAAGGAA
AAGAACGCGAGGGCAGGGCCGGCCGGTCGGTCGGTGCCTGCGCCGCACTTTTGTCATGTGCC
TAGCACAATCGAGGGCCTCACCTGCCCGCCTACCTAAAAAATAGT

Supplemental Table 1. Summary statistics of sequence-by-synthesis (SBS) small RNA and RNA-seq libraries used in this study.

(A) Number of small RNA reads from maize seedling and tassel primordium libraries by SBS sequencing.

Library	SBS reads*	Genome-matched reads†	Distinct, genome-matched reads‡	Structural RNA - matched read§
Seedling libraries				
A619 rep1 (1_A619)	19,957,581	14,067,731	3,175,417	580,505
A619 rep2 (2_A619)	26,611,750	17,062,800	3,212,249	3,355,354
A619 rep3 (3_A619)	15,413,702	13,098,107	1,483,837	598,764
fzt rep1 (1_fzt)	18,893,333	13,063,256	3,012,437	656,996
fzt rep2 (2_fzt)	16,146,074	9,308,443	2,242,646	2,746,804
fzt rep3 (3_fzt)	15,010,707	12,805,536	1,195,641	648,198
Tassel primordia libraries				
Normal sib rep1 (1T_Nsib)	25,417,120	19,300,805	4,573,444	368,094
Normal sib rep2 (2T_Nsib)	39,914,118	32,701,207	4,747,414	1,164,269
Normal sib rep3 (3T_Nsib)	31,949,641	25,972,929	5,223,978	680,557
fzt rep1 (1T_fzt)	26,803,810	19,912,137	3,847,192	470,647
fzt rep2 (2T_fzt)	42,999,370	35,204,539	4,673,353	1,109,735
fzt rep3 (3T_fzt)	31,817,065	25,180,384	5,171,764	612,867

(B) Number of RNA-seq reads from maize seedling and tassel primordium libraries by SBS sequencing.

Library	SBS reads*	Genome-matched reads†	Distinct, genome-matched reads†
Seedling libraries			
A619 rep1 (A619_mRNA_1)	48,390,153	32,986,739	13,802,327
A619 rep2 (A619_mRNA_2)	39,199,346	26,991,654	11,018,284
A619 rep3 (A619_mRNA_3)	53,171,397	32,877,538	16,772,561
A619 rep4(A619_mRNA_4)	48,833,687	30,467,909	15,048,583
fzt rep1 (fzt_mRNA_1)	46,273,586	31,177,203	13,413,861
fzt rep2 (fzt_mRNA_2)	35,970,700	22,306,804	10,943,978
fzt rep3 (fzt_mRNA_3)	51,084,786	31,971,552	15,327,774
fzt rep4 (fzt_mRNA_4)	49,832,138	30,464,416	16,195,059
Tassel primordia libraries			
Normal sib rep1 (1Tm_Nsib)	32,848,281	21,331,466	10,499,351
Normal sib rep2 (2Tm_Nsib)	44,923,665	24,888,262	14,794,347
Normal sib rep3 (3Tm_Nsib)	43,640,888	23,985,211	15,120,652
fzt rep1 (1Tm_fzt)	28,419,244	18,620,103	9,603,233
fzt rep2 (2Tm_fzt)	39,022,802	21,538,920	12,758,730
fzt rep3 (3Tm_fzt)	37,558,567	21,220,372	11,704,614

* Reads ≥ 18 bp in length (after trimming of the 3' adapter) from SBS sequencing reactions.
† Number of sequences which are matched to the genome sequence of Maize Genome Project 5b.60 AGPv2.
‡ Number of genome-matched sequences which are uniquely found within the set, excluding sequences matched to structural RNAs (t/r/sn/snoRNAs).
§ Numbers of sequences matched to structural RNAs (t/r/sn/snoRNAs).

Supplemental Table 2. Abundance of miRNAs in seedling and tassel primordium libraries. **(A)** miRNA abundances in seedling libraries.

miRNA	A619_1S	A619_2S	A619_3S	*fzt*_1S	*fzt*_2S	*fzt*_3S	Fold Change	p-value
miR398b-5p	7.11	1.16	3.21	0.00	0.00	0.07	-101.38	0.000016
miR408a-b-3p	186.20	44.36	134.16	5.27	1.53	1.18	-45.83	0.000038
miR408b-5p	7.33	0.41	1.52	0.12	0.00	0.00	-73.97	0.000156
miR394a-b-5p	193.90	4.50	15.41	2.22	0.08	0.29	-82.75	0.000168
miR167c-3p	33.14	5.04	7.38	1.17	0.32	0.37	-24.58	0.000274
miR156a-3p	6.13	3.00	4.41	0.59	0.08	0.00	-21.10	0.000795
miR167b-3p	8.98	1.77	1.85	0.47	0.00	0.07	-23.83	0.000952
miR319b,d-5p	140.64	16.42	25.28	6.32	3.70	0.59	-17.20	0.001780
miR169i-k-5p	30.30	1.84	5.94	1.52	0.40	0.29	-17.25	0.001807
miR167a-d-5p	76.16	2.93	6.74	3.51	0.48	0.59	-18.80	0.002656
miR168b-3p	53.71	3.00	7.06	2.81	0.64	0.15	-17.81	0.003027
miR168a-3p	80.05	1.36	6.02	3.04	0.16	0.07	-26.85	0.003412
miR156d,g-f-3p	108.70	18.26	35.22	9.48	2.81	1.40	-11.86	0.003446
miR398a-b-3p	27.75	10.83	32.26	5.62	0.88	1.70	-8.67	0.006280
miR528a-b-3p	50.79	2.45	9.79	4.68	0.56	0.66	-10.71	0.009762
miR156e-3p	14.14	2.11	4.65	1.76	0.40	0.22	-8.87	0.009971
miR397a-b-5p	3.52	1.91	4.97	0.94	0.08	0.37	-7.57	0.012040
miR159a-5p	26.78	1.64	2.81	2.57	0.32	0.37	-9.63	0.014022
miR2118b	15.93	2.45	2.89	1.40	1.29	0.29	-7.11	0.016870
miR399e, i-j-3p	44.29	2.79	6.82	5.15	1.45	1.33	-6.81	0.024005
miR160a-e, g-5p	648.59	10.63	27.52	56.40	3.38	6.93	-10.30	0.028673
miR398a-5p	26.56	0.48	2.65	3.28	0.40	0.22	-7.65	0.037656
miR156l-3p	57.98	13.22	21.42	12.87	4.74	4.13	-4.26	0.051517
miR156k-3p	7.78	3.75	4.73	2.11	0.64	1.25	-4.07	0.052957
miR164b-3p	15.49	0.61	2.09	2.46	0.64	0.52	-5.05	0.063800
miR164c,h-3p	15.34	0.07	2.81	1.40	1.37	0.00	-6.55	0.072312
miR167e-3p	12.04	1.02	2.09	2.81	0.40	0.44	-4.18	0.093978
miR166j-k,n-3p	411.15	15.81	82.57	71.73	33.21	7.96	-4.51	0.094014
miR444a-b	183.06	9.06	22.95	36.86	7.96	2.06	-4.59	0.096759
miR159a-b,f,j-k-3p	247.54	52.95	88.66	72.67	22.60	10.03	-3.70	0.108699
miR396a-b-3p	4.19	2.52	6.18	1.87	1.61	0.66	-3.11	0.110868
miR319a-d-3p	411.97	13.76	24.63	63.19	30.31	2.29	-4.70	0.112358
miR166a-5p	3.74	4.91	6.74	2.11	1.77	1.25	-3.00	0.114763
miR827-3p	996.60	30.46	43.81	190.85	17.77	17.84	-4.73	0.118812
miR169f-h-5p	10.85	0.48	1.20	2.81	0.32	0.29	-3.69	0.147126
miR169c-3p	16.53	6.95	19.74	8.78	4.50	1.99	-2.83	0.150224
miR160g-b-3p	10.10	0.34	0.64	2.22	0.48	0.37	-3.62	0.152030
miR156k-5p	28.13	4.16	14.04	9.83	2.49	4.13	-2.82	0.167111

miR156h-3p	7.41	1.02	1.36	1.52	1.53	0.15	-3.06	0.169994
miR164a-d,g-5p	116.18	1.91	8.10	31.83	3.70	2.80	-3.29	0.204619
miR171d-e,i-j-3p	95.61	6.61	20.86	33.11	6.83	4.20	-2.79	0.215852
miR167e-j-5p	345.69	53.15	86.90	119.94	33.29	25.07	-2.72	0.219239
miR166g-5p	3.82	0.14	0.80	5.38	8.20	0.37	2.92	0.223596
miR528a-b-5p	37.40	7.09	26.64	21.76	4.50	2.51	-2.48	0.241688
miR168a-b-5p	5793.92	459.07	641.51	1622.98	615.95	246.84	-2.77	0.254964
miR390a-b-5p	329.01	10.63	69.73	106.48	33.85	13.79	-2.66	0.267478
miR396a-b-5p	258.76	16.42	52.48	65.64	51.95	14.08	-2.49	0.273774
miR166c-5p	6.88	2.93	5.46	3.28	3.22	1.11	-2.01	0.321000
miR171d-e-5p	40.17	0.07	4.49	11.82	5.39	0.37	-2.55	0.347901
miR393a,c-5p	5.31	0.68	1.52	2.11	1.13	0.59	-1.97	0.371809
miR529-3p	8.90	0.20	0.88	2.34	2.17	0.37	-2.05	0.409106
miR169c,r-5p	10.32	0.61	1.20	5.27	0.40	0.07	-2.13	0.422256
miR156a-i,l-5p	2729.61	416.82	1265.69	1076.52	951.58	301.77	-1.89	0.433263
miR166b,d-5p	76.16	34.34	44.69	47.39	31.36	14.52	-1.66	0.480683
miR396e-f-5p	99.20	22.08	91.95	188.98	107.75	51.98	1.64	0.521011
miR156b-3p	49.45	3.88	10.27	19.31	17.61	0.44	-1.70	0.535738
miR529-5p	882.37	18.60	43.97	254.97	276.29	11.72	-1.74	0.566813
miR166l-m-3p	444.14	16.22	81.44	213.67	118.20	33.40	-1.48	0.647884
miR166n-5p	4.49	0.00	1.28	1.64	2.89	0.00	-1.27	0.813295
miR166a-3p	41600.11	11994.81	20767.72	38845.89	29647.07	11135.22	1.07	0.934536
miR396f-3p	2.17	0.27	1.69	2.22	1.85	0.29	1.05	0.946778
miR166m-5p	5.01	0.00	0.24	2.11	2.89	0.00	-1.05	0.962411
miR166b-i-3p	406.81	44.63	115.79	311.02	182.05	56.33	-1.03	0.968487

(B) miRNA abundances in tassel primordium libraries.

miRNA	Normal_1T	Normal_2T	Normal_3T	*fzt*_1T	*fzt*_2T	*fzt*_3T	Fold Change	p-value
miR167d-3p	6.89	3.92	4.96	0.22	0.04	0.09	-45.32	1.00E-05
miR167a-d-5p	63.01	58.56	58.52	2.91	1.57	1.53	-29.98	1.11E-05
miR172e	5.45	3.40	2.61	0.15	0.12	0.09	-30.68	2.74E-05
miR408a-b-3p	1.36	35.03	22.82	0.22	0.20	0.74	-49.87	6.87E-05
miR398b-5p	0.00	4.38	6.42	0.07	0.00	0.09	-60.85	0.000371
miR394a-b-5p	41.20	24.90	33.45	4.14	0.56	0.79	-18.21	0.000421
miR167c-3p	41.50	50.99	73.81	2.62	6.05	6.54	-10.91	0.001073
miR398a-b-3p	0.23	33.75	32.74	0.15	1.33	2.27	-17.63	0.004924
miR319a-d-3p	307.12	170.02	181.97	70.76	12.78	9.00	-7.12	0.009999
miR159a-b,f,j-k-3p	240.92	327.02	219.73	27.53	91.81	45.35	-4.78	0.021724
miR528a-b-5p	6.06	52.82	34.00	0.58	5.32	8.39	-6.48	0.023661
miR160a-e,g-5p	18.78	15.19	10.03	1.96	3.79	3.34	-4.82	0.028341
miR166j-k,n-3p	1063.06	759.47	709.03	310.14	211.85	230.71	-3.36	0.038039
miR159a-5p	141.78	11.24	14.99	23.32	0.73	2.55	-6.32	0.045364

miR444a-b	20.30	11.83	11.98	3.71	3.39	5.56	-3.48	0.076749
miR399e,i-j-3p	24.92	0.38	0.80	4.36	0.40	0.14	-5.34	0.101966
miR528a-b-3p	0.23	14.51	9.68	0.00	2.74	3.66	-3.80	0.171741
miR529-5p	28586.87	5313.93	2203.75	13007.52	1168.54	1340.79	-2.33	0.196562
miR166c-5p	13.78	5.92	4.41	5.96	2.34	1.21	-2.54	0.201334
miR166a-3p	57911.96	13792.38	7356.52	29633.78	5468.07	4890.56	-1.98	0.212390
miR168a-3p	15.75	0.47	0.35	4.07	0.77	0.00	-3.43	0.241722
miR166b,d-5p	109.74	54.99	24.32	60.88	13.47	11.22	-2.21	0.280910
miR171d-e,i-j-3p	16.81	11.49	9.88	8.86	4.80	5.84	-1.96	0.330129
miR390a-b-5p	166.02	26.17	28.78	78.24	9.84	15.07	-2.14	0.330370
miR397a-b-5p	0.08	4.85	4.21	0.00	1.77	2.27	-2.25	0.383805
miR171d-e-5p	20.15	8.13	8.57	12.64	3.79	4.59	-1.75	0.432998
miR164g-3p	22.27	4.89	12.79	49.18	7.94	9.78	1.67	0.487308
miR168b-3p	19.31	0.47	0.30	9.44	0.44	0.05	-2.02	0.505393
miR166n-5p	176.32	37.66	40.57	127.06	9.84	17.39	-1.65	0.525309
miR396a-b-5p	79.15	2.98	2.61	43.01	1.49	1.81	-1.83	0.525607
miR156a-i,l-5p	2.50	1.28	1.30	2.62	0.20	0.14	-1.73	0.535494
miR319b,d-5p	3.48	0.04	0.15	6.54	0.04	0.00	1.79	0.617197
miR166k-5p	76.95	9.45	10.68	54.56	4.64	6.12	-1.49	0.625897
miR529-3p	604.77	15.24	12.69	983.89	6.81	7.47	1.58	0.660026
miR390a-b-3p	4.47	1.79	0.80	3.85	1.01	0.70	-1.27	0.741551
miR160b,g-3p	12.95	0.98	1.60	10.53	0.52	0.70	-1.32	0.751210
miR166l-m-3p	1619.05	816.50	659.43	1492.73	577.35	539.46	-1.19	0.765345
miR166b-3p	1039.80	172.07	100.94	905.21	70.64	75.08	-1.25	0.774307
miR827-3p	58.24	40.60	91.66	88.12	31.61	42.85	-1.17	0.814654
miR164a-3p	9.47	0.94	1.45	9.08	0.81	0.51	-1.14	0.876787
miR166m-5p	34.69	16.60	10.03	46.79	13.43	8.21	1.12	0.877797
miR396e-f-5p	1.59	0.51	1.50	2.03	0.32	1.72	1.13	0.883789
miR164a-d,g-5p	15.15	8.30	6.62	19.11	3.67	4.54	-1.10	0.894511
miR166a-5p	20.90	9.62	5.37	28.04	6.17	4.92	1.09	0.907698
miR168a-b-5p	319.69	159.43	141.10	435.17	107.13	96.78	1.03	0.964328

Supplemental Table 3. Abundance of pri-miRNAs in seedling and tassel primordium libraries. **(A)** pri-miRNA abundances in seedling libraries.

pri-miRNA	A619 1S	A619 2S	A619 4S	A619 5S	fzt_1S	*fzt*_2S	*fzt*_4S	*fzt*_5S	log_2FC	p-value	FDR
pri-miRNA 528b	0.09	1.72	1.50	1.58	4.67	7.86	18.50	5.60	2.91	2.33E-23	5.99E-21
pri-miRNA 156b	3.46	1.08	0.20	0.52	5.24	7.82	0.39	20.88	2.71	8.06E-21	1.66E-18
pri-miRNA 319b	1.13	1.96	5.51	3.45	10.97	7.59	15.29	20.44	2.17	3.47E-15	4.47E-13
pri-miRNA 167d	0.07	0.46	0.64	0.28	1.62	1.65	1.58	3.51	2.51	2.64E-14	3.12E-12
pri-miRNA 167c	0.06	0.08	0.31	0.11	0.56	0.20	1.72	1.24	2.68	1.19E-11	9.92E-10
pri-miRNA 528a	0.03	1.41	1.07	1.54	2.20	4.05	7.88	1.81	1.98	1.27E-11	1.05E-09
pri-miRNA 159a	16.33	17.71	16.23	13.57	42.27	32.64	44.41	93.96	1.74	4.66E-11	3.52E-09
pri-miRNA 408b	0.17	2.28	2.17	3.83	6.02	7.51	12.39	3.02	1.77	1.53E-10	1.08E-08
pri-miRNA 169c	1.22	2.12	7.69	13.30	5.62	8.49	33.64	19.24	1.46	3.99E-08	1.84E-06
pri-miRNA 168b	4.10	4.16	5.16	4.02	8.81	7.67	15.55	14.48	1.41	1.34E-07	5.60E-06
pri-miRNA 172c	1.60	3.60	2.12	1.90	4.70	3.95	6.48	8.98	1.39	4.53E-07	1.69E-05
pri-miRNA 159f	2.82	3.52	4.13	5.33	8.68	6.76	11.38	12.14	1.30	1.24E-06	4.15E-05
pri-miRNA 398b	0.29	8.63	6.50	13.98	7.60	17.19	36.90	7.28	1.23	3.12E-06	9.42E-05
pri-miRNA 166h	2.06	0.88	0.47	0.49	1.95	3.28	0.82	3.67	1.32	7.69E-06	0.000207
pri-miRNA 156f	16.62	14.67	23.86	20.61	37.97	24.78	47.51	52.22	1.10	2.33E-05	0.000555
pri-miRNA 168a	12.03	12.03	22.52	16.02	34.70	28.81	35.71	33.85	1.09	2.99E-05	0.000685
pri-miRNA 397a	0.67	1.28	0.02	1.11	0.31	0.75	0.00	0.56	-0.91	0.007992	0.075175
pri-miRNA 156g	20.95	32.45	39.62	39.46	71.34	42.29	44.08	47.38	0.63	0.014359	0.117918
pri-miRNA 169d	0.09	1.72	9.87	8.48	2.75	2.81	19.10	5.13	0.56	0.033946	0.218638
pri-miRNA 169b	0.09	1.32	1.50	1.50	0.43	2.53	2.42	1.22	0.59	0.046887	0.270172
pri-miRNA 156l	0.65	0.50	0.43	1.06	0.67	1.93	1.06	0.12	0.52	0.102654	0.440367
pri-miRNA 162	1.74	1.68	3.59	4.89	1.70	0.75	3.86	2.63	-0.41	0.134327	0.512222
pri-miRNA 164b	3.63	3.48	5.29	4.98	3.46	5.61	7.32	6.40	0.39	0.142310	0.528950
pri-miRNA 167b	1.83	1.68	3.66	2.42	2.35	2.65	5.77	1.36	0.34	0.220493	0.658025
pri-miRNA 399g	62.62	70.74	109.74	138.01	47.67	90.11	70.95	98.00	-0.31	0.220984	0.658383
pri-miRNA 396d	0.87	2.20	1.81	4.30	2.44	1.98	3.63	3.48	0.33	0.232499	0.674695
pri-miRNA 169h	0.33	0.71	1.53	0.88	0.65	0.21	1.36	0.57	-0.31	0.327345	0.770845
pri-miRNA 396c	0.41	0.53	1.71	2.39	1.10	0.83	2.19	1.87	0.25	0.398249	0.820271
pri-miRNA 396a	1.51	1.80	1.81	2.23	1.85	2.25	2.42	2.08	0.23	0.420679	0.836266
pri-miRNA 169i	1.05	2.24	7.43	8.27	4.48	2.57	11.86	3.09	0.21	0.426833	0.839534
pri-miRNA 156d	31.58	21.66	20.84	21.46	36.00	22.31	29.63	19.61	0.17	0.506920	0.881953
pri-miRNA 171i	0.67	0.48	2.39	1.85	1.17	0.40	2.42	2.17	0.19	0.519809	0.887347
pri-miRNA 166d	0.78	1.40	2.14	1.60	0.93	0.91	1.92	2.80	0.14	0.624142	0.925777
pri-miRNA 166l	0.17	0.36	2.86	2.07	0.74	0.40	3.94	0.88	0.12	0.677706	0.941492
pri-miRNA 169e	3.48	2.96	3.98	3.71	3.09	2.88	6.21	2.76	0.08	0.766577	0.962968
pri-miRNA 2275d	56.23	57.27	75.85	86.50	56.08	64.58	60.02	83.11	-0.06	0.800611	0.971546
pri-miRNA 171f	1.92	0.60	3.66	1.71	1.98	2.06	1.66	2.19	-0.01	0.981092	0.997767
pri-miRNA 156k	22.07	17.64	31.45	32.20	19.08	14.68	47.56	21.86	0.00	0.992717	0.999578

(B) pri-miRNA abundances in tassel primordium libraries.

pri-miRNA	Normal 1T	Normal 2T	Normal 3T	*fzt*_1T	*fzt*_2T	*fzt*_3T	log_2FC	p-value	FDR
pri-miRNA 167d	20.19	16.23	36.04	130.87	196.14	248.56	2.99	7.18E-21	4.63E-18
pri-miRNA 167c	4.78	4.99	14.90	29.32	56.98	80.05	2.75	6.09E-18	2.46E-15
pri-miRNA 172e	13.93	12.60	33.98	63.05	155.75	152.14	2.62	9.18E-17	3.36E-14
pri-miRNA 168a	1.83	2.14	4.33	7.25	19.02	17.58	2.40	1.38E-13	3.39E-11
pri-miRNA 156f	1.95	1.44	0.77	0.34	0.03	0.07	-3.24	1.19E-11	2.08E-09
pri-miRNA 408b	0.21	14.28	22.72	0.29	76.97	73.26	2.02	7.27E-11	1.15E-08
pri-miRNA 528b	0.33	25.50	53.77	0.19	108.26	206.55	1.98	1.05E-10	1.61E-08
pri-miRNA 319d	0.08	0.18	0.03	0.72	1.08	1.17	3.29	3.86E-10	5.42E-08
pri-miRNA 159f	15.22	7.61	11.88	38.19	42.45	42.62	1.83	2.92E-09	3.53E-07
pri-miRNA 166k, m	1.83	2.56	4.47	4.37	15.44	12.12	1.85	7.45E-09	8.55E-07
pri-miRNA 159d	0.46	0.15	0.18	1.97	1.53	0.77	2.44	1.55E-08	1.72E-06
pri-miRNA 156d	2.08	1.94	0.59	0.48	0.24	0.17	-2.36	2.03E-08	2.20E-06
pri-miRNA 528a	0.04	18.82	21.73	0.10	50.31	69.68	1.56	3.01E-07	2.61E-05
pri-miRNA 171e	0.12	0.03	0.44	0.48	1.36	1.10	2.29	8.43E-07	6.60E-05
pri-miRNA 394a	3.45	5.11	6.16	7.53	16.10	17.68	1.49	1.81E-06	0.000133
pri-miRNA 172c	14.30	12.87	16.77	41.74	44.61	32.58	1.44	2.32E-06	0.000167
pri-miRNA 159a	163.54	142.56	271.55	331.21	480.47	649.41	1.34	8.05E-06	0.000503
pri-miRNA 169b	2.04	2.44	2.22	0.72	0.80	0.80	-1.52	2.69E-05	0.001462
pri-miRNA 168b	7.44	7.00	8.98	14.84	20.18	18.92	1.20	8.46E-05	0.004029
pri-miRNA 398b	0.25	132.54	121.23	0.10	291.83	277.80	1.17	9.79E-05	0.004559
pri-miRNA 166d	6.65	3.88	3.41	1.87	2.89	2.38	-0.96	0.002889	0.079827
pri-miRNA 319a	0.58	0.71	1.42	1.49	1.67	2.52	1.06	0.003106	0.084519
pri-miRNA 390a	3.41	3.06	5.48	4.70	9.91	7.80	0.91	0.003675	0.096527
pri-miRNA 171j	1.00	0.76	1.75	1.82	2.02	3.15	0.99	0.004325	0.110282
pri-miRNA 319c	0.30	0.50	0.53	0.48	1.39	1.05	1.13	0.005876	0.139716
pri-miRNA 156k	6.95	9.79	5.51	4.27	4.00	4.29	-0.83	0.008170	0.181083
pri-miRNA 394b	1.95	1.38	1.54	1.44	3.23	2.80	0.62	0.066206	0.760186
pri-miRNA 164d	0.62	0.73	0.53	0.48	1.46	1.07	0.67	0.084092	0.869147
pri-miRNA 169h	2.48	1.26	1.17	3.02	2.17	2.00	0.55	0.103341	0.967291
pri-miRNA 156g	1.91	1.94	1.21	1.44	1.11	0.90	-0.55	0.118805	0.999993
pri-miRNA 395d,f,g	0.08	0.29	2.67	0.10	0.80	1.17	-0.55	0.154137	0.999993
pri-miRNA 167b	8.03	7.23	6.19	8.97	11.61	8.07	0.42	0.170673	0.999993
pri-miRNA 171d	0.67	1.18	1.60	0.29	0.97	1.21	-0.48	0.203909	0.999993
pri-miRNA 395a	0.46	0.94	3.79	0.24	1.70	1.94	-0.41	0.238072	0.999993
pri-miRNA 169e	14.82	6.87	6.83	16.75	11.32	7.78	0.33	0.276094	0.999993
pri-miRNA 399g	178.64	191.45	167.18	151.38	211.38	124.65	-0.14	0.634086	0.999993
pri-miRNA 2275d	91.36	75.33	69.59	76.19	83.93	59.56	-0.10	0.722512	0.999993
pri-miRNA 529	24.42	20.04	15.46	27.87	10.27	25.89	0.10	0.750200	0.999993
pri-miRNA 162	3.59	9.81	10.55	4.27	7.27	12.94	0.03	0.921054	0.999993

Supplemental Table 4: Summary of predicted miRNA targets based on conserved biological function in *dcl1-fzt* and normal tassel primordia. Differentially expressed targets are indicated in bold

Gene ID	Locus	mF Score	Log(2) CPM	Log(2) FC	P value	FDR
miR159a-b,f,j-k-3p (PF00249: Myb-like DNA binding domain)						
GRMZM2G423833	***myb115***	2	2.8753	**1.0470**	**0.00082**	**.01443**
GRMZM2G093789	*mmyb59*	2.5	4.4846	0.8587	0.00427	0.0565
GRMZM2G004090	*myb87*	2.5	-0.007	0.5005	0.20567	0.7919
GRMZM2G028054	*myb74*	3	3.2294	-0.0257	0.93313	0.9999
GRMZM2G139688	***myb138***	3.5	3.4013	**1.7189**	**4.75E-08**	**2.38E-06**
GRMZM2G049194	*mybr67*	5.5	1.5715	-0.7996	0.01646	0.1581
GRMZM2G050550	***myb153***	6	2.8898	**1.7955**	**2.19E-08**	**1.17E-06**
GRMZM2G130149	*myb56*	6.5	3.3538	-0.1965	0.51900	0.9999
miR160a-e,g-50 (PF02309; PF02362; PF06507: B3 DNA binding domain; Auxin response factor; AUX/IAA family)						
GRMZM2G153233	*arftf2*	1	5.3861	5.3861	0.5516	0.0641
GRMZM2G159399	*arftf17*	1	5.4598	0.4698	0.1144	0.5796
AC207656.3_FG002	*arftf19*	1	0.9716	-0.2670	0.4416	0.9999
GRMZM5G808366	*arftf5*		1.2607	-0.1147	0.7338	0.9999
GRMZM2G081406	*arftf15*	2	4.1355	0.6909	0.0222	0.1967
GRMZM2G338259	*arftf10*	6.5	8.6898	0.1590	0.5895	0.9999
GRMZM5G874163	*arftf26*	7	6.15093	0.07146	0.8092	0.9999
miR167a-d-5p (PF02309; PF02362; PF06507: B3 DNA binding domain; Auxin response factor; AUX/IAA family)						
GRMZM2G475882	*arftf30*	4	6.5423	0.6427	0.0304	0.2458
GRMZM2G078274	*arftf3*	4	7.6643	0.3617	0.2208	0.8131
GRMZM2G081158	***arftf34***	**5**	**8.4320**	**1.6456**	**5.33E-08**	**2.65E-06**
GRMZM2G073750	***arftf9***	**5**	**6.4322**	**1.0271**	**0.0006**	**0.0109**
GRMZM2G089640	*arfrf22*	5	6.4787	0.6851	0.0211	0.1898
GRMZM2G028980	*arftf16*	5	7.3120	0.4336	0.1426	0.6586
GRMZM2G035405	*arftf18*	5	7.1127	0.02455	0.93374	0.9999
GRMZM2G086949	*arftf29*	5.5	4.6541	-0.8669	0.0040	0.05343
GRMZM2G034840	***arftf4***	**6.5**	**5.0653**	**-1.4576**	**1.67E-06**	**6.19E-05**
miR172e (PF0847: AP2 domain)						
GRMZM2G160730	***gl15***	**2**	**0.02606**	**1.2209**	**0.0017**	**0.0265**

Gene ID	Locus	mF Score	Log(2) CPM	Log(2) FC	P value	FDR
GRMZM5G862109	***ids1***	**2.5**	**5.5508**	**0.9674**	**0.0012**	**0.0206**
GRMZM2G176175	*ereb121*	2.5	4.7519	0.8321	0.0056	0.0701
GRMZM2G174784	***ereb197***	**3**	**3.2165**	**1.0892**	**0.0004**	**0.0086**
GRMZM2G076602	*ereb212*	3	0.7817	0.5001	0.1586	0.6973
GRMZM2G124524	*wri1*	4	2.4794	0.09893	0.7521	0.9999
GRMZM2G020054	*ereb54*	6.5	1.3410	-0.0462	0.8904	0.9999
miR319a-d-3p (PF03634: TCP family transcription factor)						
GRMZM2G148022	*tcptf29*	2.5	0.8043	-0.9688	0.0069	0.0811
GRMZM2G089361	*tcptf44*	2.5	2.0622	0.2813	0.3791	0.9689
GRMZM2G115516	*tcptf5*	2.5	2.5601	0.1603	0.6077	0.9999
GRMZM2G020805	*tcptf43*	3	2.1055	0.4581	0.1516	0.6816
GRMZM2G015037	*tcptf24*	4	3.1169	0.1239	0.6860	0.9999
miR394a-b-5p (PF00646: F-box domain)						
GRMZM2G119650		**0**	**6.7312**	**1.0151**	**0.0007**	**0.0122**
GRMZM2G064954		**0**	**6.0225**	**0.8676**	**0.0036**	**0.0495**
miR408a-b-3p (PF2298, PF00732: plastocyanin-like domain, multicopper oxidase)						
GRMZM2G004012		2.5	5.3719	0.4958	0.0959	0.5205
GRMZM2G352678		3.5	1.4754	-0.5048	0.1295	0.6231
GRMZM2G076225		5	2.0026	-0.1700	0.5956	0.9999
GRMZM2G177934		6.5	1.2213	0.2870	0.3966	0.9796

Supplemental Table 5. Summary of predicted miRNA targets based on conserved biological function in *dcl1-fzt* and normal seedlings. Differentially expressed targets are indicated in bold.

Gene ID	Locus	mF Score	Log(2) CPM	Log(2) FC	P value	FDR
miR160a-e,g-50 (PF02309; PF02362; PF06507: B3 DNA binding domain; Auxin response factor; AUX/IAA family)						
GRMZM2G153233	***arftf2***	**1**	**4.9775**	**0.9625**	**0.0002**	**0.0029**
GRMZM2G159399	*arftf17*	1	4.7477	0.6050	0.01925	0.1126
AC207656.3_FG002	***arftf19***	**1**	**4.3744**	**0.9749**	**0.0002**	**0.0026**
GRMZM2G390641	*arftf21*	1	0.8911	-0.3745	0.1970	0.5211
GRMZM5G808366	*arftf5*	1.5	-0.3870	0.1681	0.6166	0.8655
GRMZM2G081406	***artff15***	**2**	**2.7105**	**-1.701**	**5.60E-10**	**2.61E-08**
GRMZM2G328742	*abi40*	4	1.0133	-0.4354	0.1300	0.4117
GRMZM2G338259	*arftf10*	6.5	7.3086	0.0565	0.8250	0.9500
GRMZM5G874163	*arftf26*	7	5.0434	0.2918	0.0.2567	0.5990
miR167a-d-5p (PF02309; PF02362; PF06507: B3 DNA binding domain; Auxin response factor; AUX/IAA family)						
GRMZM2G475882	*arftf30*	4	4.6187	0.3398	0.1878	0.5064
GRMZM2G078274	*arftf3*	4	5.9387	0.2996	0.2425	0.5816
GRMZM2G035405	***arftf18***	**5**	**5.9680**	**0.7376**	**0.0042**	**0.0349**
GRMZM2G081158	*arftf34*	5	5.966	0.3969	0.1218	0.3957
GRMZM2G073750	*arftf9*	5	4.4693	-0.3912	0.1300	0.4118
GRMZM2G089640	*arftf22*	5	4.6208	0.0912	0.7235	0.9119
GRMZM2G028980	*arftf16*	5	6.0209	0.3570	0.1638	0.4707
GRMZM2G086949	*arftf29*	5.5	0.6835	0.1894	0.5202	0.8158
GRMZM2G034840	*arftf4*	6.5	1.764	-0.3944	0.1510	0.4501
miR169i-k5p (PF002045: CCAAT-binding transcription factor)						
GRMZM5G857944	*ca2p13*	2	3.8294	0.6390	0.0143	0.0897
GRMZM2G091964	***ca2p16***	**3**	**4.0559**	**1.1589**	**1.03E-05**	**0.0002**
GRMZM2G000686	***ca2p11***	**3**	**3.0994**	**0.9387**	**0.0004**	**0.0050**
GRMZM2G165488	*ca2p10*	3	0.9833	0.5327	0.0648	0.2668
GRMZM5G829103	*ca2p6*	3	0.2371	0.3788	0.2201	0.5544
GRMZM5G853836	*ca2p5*	3	2.9136	-0.2861	0.2784	0.6231
GRMZM2G037630	*ca2p3*	3.5	2.123	0.2441	0.3661	0.7076
GRMZM2G040349	***ca2p4***	**4**	**0.9044**	**0.8296**	**0.0045**	**0.0371**
GRMZM2G038303	*ca2p15*	4	0.9956	0.2292	0.4249	0.7537
miR394a-b-5p (PF00646: F-box domain)						
GRMZM2G119650		**0**	**6.9199**	**0.9476**	**0.0002**	**0.0032**
GRMZM2G064954		**0**	**5.611**	**0.7569**	**0.0033**	**0.0291**
miR397a-b-5p (PF007732, PF00394, PF7731: Multicopper oxidase)						
GRMZM2G072808		**0**	**5.2327**	**-1.222**	**2.79E-06**	**6.48E-05**

Gene ID	Locus	mF Score	Log(2) CPM	Log(2) FC	P value	FDR
GRMZM2G305526		**4**	**3.1111**	**-2.2761**	**2.62E-16**	**2.59E-14**
GRMZM2G447271		**4**	**3.5578**	**-1.1218**	**2.19E-05**	**0.0004**
GRMZM2G146152		**4.5**	**4.7830**	**-0.9074**	**0.0005**	**0.0057**
GRMZM2G132169		6	7.0000	-0.2284	0.3717	0.7120
GRMZM2G336337		6	5.4715	-0.0256	0.9206	0.9798
GRMZM2G367668		**7**	**5.3805**	**-1.5703**	**2.35E-09**	**9.90E-08**
GRMZM2G388587		**7**	**1.1616**	**-0.7611**	**0.0063**	**0.0479**
GRMZM2G094375		7	3.3346	-0.5501	0.0362	0.1773
miR408a-b-3p (PF2298, PF00732: plastocyanin-like domain, multicopper oxidase)						
GRMZM5G866053		2	2.0237	-0.65174	0.0167	0.1013
GRMZM2G004012		2.5	2.0464	0.3490	0.1981	0.5225
GRMZM2G023847		3	6.3529	0.1348	0.5985	0.8558
GRMZM2G352678		**3.5**	**3.9382**	**-0.7466**	**0.0042**	**0.0352**
GRMZM2G097851		3.5	5.2463	-0.1514	0.5553	0.8347
GRMZM5G814718		4	3.9293	-0.1072	0.6794	0.8935
GRMZM2G336337		4	5.4715	-0.2557	0.9206	0.9798
GRMZM2G132169		4.5	7.0003	-0.2284	0.3717	0.7120
GRMZM2G076225		5	0.8160	-0.7983	0.0067	0.05037
GRMZM2G043300		5	4.0512	-0.5639	0.0300	0.1555
GRMZM2G053779		5	4.6357	0.1549	0.5479	0.8310
GRMZM2G039381		6	1.8140	-0.3881	0.1566	0.4561
GRMZM2G177934		**6.5**	**0.3775**	**0.9964**	**0.0012**	**0.0130**

Supplemental Table 6: Primers used in this study.

Primer Name	Sequence
ZmGAPDF-5F	CCTGCTTCTCATGGATGGTT
ZmGAPDF-6R	TGGTAGCAGGAAGGGAAACA
GRMZM2G475882-2F	TGTCGCATCGAAATCTTCAG
GRMZM2G475882-2R	TTGCAGTTCATCGTCGAAAG
GRMZM2G078274-2F	TGTGTCGCATCAGGATCTTC
GRMZM2G078274-2R	TTGCAGTTCATCGTCGAAAG
GRMZM2G119650-4F	TGACAAGTTCTGCGAAAACG
GRMZM2G119650-4R	ACTCAGCTCTGGGCAGGTAA
GRMZM2G004012-5F	CGTGTAGGCTCAGTCAGTCG
GRMZM2G004012-5R	CGTCAAGCAATTTGTCATGG
GRMZM2G423833-1F	GTTCCTGAGCAGCAGTTTCC
GRMZM2G423833-2R	GCTCATCATCCCAGCAAAGT
GRMZM2G150893-1F	TGATTAATCCACGACGACGA
GRMZM2G150893-1R	CGCTAGTGCACTCTTGCTTG
GRMZM5G832582-2F	TCGTGGAAAGACTGGGATTC
GRMZM5G832582-1R	GTCAGCAAGGCAACTCTTCC
GRMZM2G074238-2F	TCCAGGTCGTCACGTGTAGT
GRMZM2G074238-2R	GCATCCTAGCTACAACGCTAGA
GRMZM2G081158-3F	CAGGCAAGGCAAGAATTGAT
GRMZM2G081158-2R	GAAAGAATCGGCAAAGGTGA
GRMZM2G139688- 2F	CAGGTGCAGCAGCTACCATA
GRMZM2G139688- 2R	TGACAGGGTTGACAAAAACG
GRMZM2G352678-2F	TCGTGTGGCATACTCGTACC
GRMZM2G352678-2R	CCATCAGCCACACGTACATC
GRMZM5G899308-2F	GTCCGGCGTAGTTTCTTGAG
GRMZM5G899308-2R	TGGATTATTGGTTCGGCTTC
GRMZM5G803935-2F	TTGATGATGCTGCATTGGAT
GRMZM5G803935-2R	TAGCAAGCCTGGAAGGAAGA